

# Compilation for Surface Code Quantum Computers

ABTIN MOLAVI, University of Wisconsin-Madison, USA

AMANDA XU, University of Wisconsin-Madison, USA

SWAMIT TANNU, University of Wisconsin-Madison, USA

AWS ALBARGHOUTHI, University of Wisconsin-Madison, USA

Practical applications of quantum computing depend on fault-tolerant devices with error correction. Today, the most promising approach is a class of error-correcting codes called surface codes. In this paper, we study the problem of compiling quantum circuits for quantum computers implementing surface codes. The problem involves (1) *mapping* circuit qubits to the device qubits and (2) *routing* execution paths between pairs of interacting qubits. We call this the *surface code mapping and routing* problem (scmr).

Solving scmr near-optimally is critical for both efficiency and correctness. An optimal solution limits the cost of a computation in terms of precious quantum resources and also minimizes the probability of incurring an undetected logical error, which increases with each additional time step.

We study scmr from a theoretical and practical perspective. First, we prove that scmr, as well as a constrained version of the problem, is NP-complete. Second, we present a optimal algorithm for solving scmr that is based on a SAT encoding. Third, we present a spectrum of efficient relaxations of scmr, for example, by exploiting greedy algorithms for solving the problem of *node-disjoint paths*. Finally, we implement and evaluate our algorithms on a large suite of real and synthetic circuits. Our results suggest that our relaxations are a powerful tool for compiling realistic workloads. The relaxation-based algorithms are orders of magnitude faster than the optimal algorithm (solving instances with tens of thousands of gates in minutes), while still finding high-quality solutions, achieving the theoretical lower bound on up to 55 out of 168 circuits from a diverse benchmark suite.

## 1 INTRODUCTION

Quantum computation promises to surpass classical methods in optimization and simulation with the potential to unlock breakthroughs in materials science, chemistry, machine learning and beyond. However, since individual physical qubits and quantum operations are error-prone, these long-term applications require an error-correction scheme for detecting and correcting faults. Quantum error-correction achieves acceptable error rates with redundancy: encoding the state of a single logical qubit into several physical qubits. Experimentalists have recently demonstrated error suppression for a single logical qubit [1, 38, 49], and multi-qubit systems are expected to follow soon.

In order to harness the full power of the fault-tolerant quantum computers on the horizon, we need optimizing compilers that convert circuit-level descriptions of quantum programs to error-corrected elementary operations while preserving as much parallelism as possible. The focus of this work is to answer the following question:

*How can we compile a given circuit for a fault-tolerant device such that execution time is minimized?*

In particular, we target a well-studied type of error-correction scheme called a *surface code* [18, 27, 32]. A surface-encoded quantum device embeds qubits into a large two-dimensional grid. Two-qubit gates impose limitations on the execution of a quantum circuit by introducing contention constraints. Each two-qubit gate occupies a path on the grid and simultaneous paths cannot cross. Gates which can theoretically be executed in parallel may be forced into sequential execution if the path of one spatially “blocks” the other. Therefore, to maximize computational throughput and minimize the probability of accumulating a logical error over the course of a computation, a

---

Authors' addresses: Abtin Molavi, University of Wisconsin-Madison, Madison, WI, USA, [amolavi@wisc.edu](mailto:amolavi@wisc.edu); Amanda Xu, University of Wisconsin-Madison, Madison, WI, USA, [axu44@wisc.edu](mailto:axu44@wisc.edu); Swamit Tannu, University of Wisconsin-Madison, Madison, WI, USA, [stannu@wisc.edu](mailto:stannu@wisc.edu); Aws Albarghouthi, University of Wisconsin-Madison, Madison, WI, USA, [aws@cs.wisc.edu](mailto:aws@cs.wisc.edu).

compiler must carefully *map* qubits to grid locations and *route* two-qubit gates. While some recent study of surface code architectures and compilers has considered variants of this compilation pass [8, 23, 25, 46], its optimization in full generality remains largely unaddressed.

In this paper, we study the problem, which we call *surface code mapping and routing* (SCMR), from a theoretical and algorithmic perspective. We begin by understanding its hardness. We show that surface code mapping and routing is NP-complete via a reduction from a classical job scheduling problem. The key idea is that we can encode an arbitrary job dependency structure into a quantum circuit such that an optimal job schedule corresponds to an optimal execution order for the circuit. Next, we present a natural SAT encoding of the problem that is guaranteed to provide an optimal solution.

We then study a spectrum of relaxations to the SCMR problem, by breaking it into independent mapping and routing steps. We compare two mapping strategies. One is circuit-independent, taking a randomized ensemble of mappings and keeping the one that results in the best solution. The other is based on a heuristic that places interacting qubits in adjacent locations to minimize conflict. For routing, we observe this subproblem is similar to an existing graph-theoretic problem, originally motivated by VLSI routing [3, 29], called Node-Disjoint Paths [26]. The connection to Node-Disjoint Paths allows us to leverage an existing  $O(\sqrt{n})$ -approximation algorithm as a subroutine and extend it to a simple greedy routing algorithm with a guaranteed approximation ratio.

Finally we provide an implementation of each of these algorithms and a thorough evaluation. We consider a comprehensive suite of benchmarks consisting of over 100 application circuits implementing important quantum algorithms, along with procedurally-generated synthetic circuits. Some of these synthetic circuits are designed to have a known optimal solution, allowing us to precisely assess the quality of solutions for arbitrarily large circuits. Overall, our findings highlight the power of our relaxations, which deliver near-optimal solutions while scaling to architectures with hundreds of logical qubits and circuits with nearly 100,000 gates.

**Contributions.** We summarize our contributions as follows:

- A formal definition of the surface code mapping and routing problem (SCMR) using an abstraction that captures the central combinatorial challenge in compiling quantum circuits for surface code devices (Section 3).
- A proof of the NP-completeness of the SCMR problem (Section 4).
- An optimal SCMR solver based on an exact SAT encoding (Section 5).
- A spectrum of approximate solvers based on heuristic mapping strategies and an approximation algorithm for routing (Section 6).
- An extensive empirical evaluation that demonstrates the utility of our relaxations and provides insights into their relative strengths (Section 8).

## 2 SURFACE CODE COMPIRATION: AN ILLUSTRATED PRIMER

In this section, we describe the surface code mapping and routing problem and present a few illustrative examples. The basics of error-corrected quantum computation are presented in Section 2.1 primarily to provide some intuition behind the constraints of the problem. In Section 2.2 (and the rest of the paper), we mostly abstract away these details and focus on the graph-theoretic formulation of routing non-intersecting paths in a grid.

### 2.1 Quantum Circuits and Error Correction

**Qubits, gates, and circuits.** The fundamental unit of quantum computing is called the quantum bit, or qubit. The state of a qubit is described by a two-dimensional complex unit vector with basis

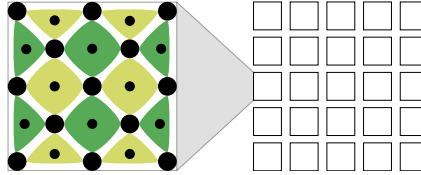


Fig. 2. Quantum device implementing a surface code with close-up view of a surface code logical qubit

states  $|0\rangle = \begin{bmatrix} 1 \\ 0 \end{bmatrix}$  and  $|1\rangle = \begin{bmatrix} 0 \\ 1 \end{bmatrix}$ . Measuring a qubit in the state  $\alpha|0\rangle + \beta|1\rangle$  collapses its state into one of the basis states:  $|0\rangle$  with probability  $|\alpha|^2$  and  $|1\rangle$  with probability  $|\beta|^2$ .

Quantum gates are unitary transformations on the state of one or more qubits. The gates relevant to this work are the one-qubit T gate and the two-qubit controlled-not (CNOT) gate. The CNOT gate is not symmetric in its arguments; the first input is the *control* qubit and the second is the *target* qubit. With the addition of one gate, the Hadamard gate, we have a universal gate set, allowing us to approximate arbitrary unitary transformations to arbitrary precision. The Hadamard gate differs from the CNOT and T gates in that it can be performed “virtually” in classical control software on fault-tolerant quantum computers [33]. For this reason, we focus on executing CNOT and T gates.

A *quantum circuit* is a sequence of gate applications. A common representation of a quantum circuit is shown in Fig. 1. Each horizontal wire represents a qubit. This circuit consists of two parallel operations: a CNOT between qubits  $q_0$  and  $q_1$  and a T gate on  $q_2$ . We will sometimes refer to the *depth* of a circuit, which is the longest chain of dependent operations. This circuit has a depth of 1.

**Quantum error correction.** Physical realizations of the qubit are extremely delicate and subject to unintended changes of state due to interactions with environmental factors or energy decays, leading to errors in computation.

The leading approach to overcome these challenges is called a surface code [18]. A surface code encodes a logical qubit using a two-dimensional lattice of physical qubits; an example of a logical qubit encoded using a surface code is shown in the insert on the left of Fig. 2. Each physical qubit in the lattice is designated as either a data qubit (large circles in the figure) or a measurement qubit (small circle). Data qubits carry the state of the logical qubit, whereas measurement qubits are repeatedly measured to detect errors. There are two types of measurement qubits (indicated by color of the surrounding region in the figure) to detect the two classes of qubit error: bit-flips and phase-flips.

As depicted on the right of Fig. 2, multiple surface code logical qubits can be encoded into one large lattice of physical qubits as long as they are separated by a buffer of physical qubits, represented by the gaps between squares.

## 2.2 Surface Code Mapping and Routing by Example

We will now introduce the surface code mapping and routing problem by developing some examples. The grid from Fig. 2 will be our quantum computing architecture. The logical qubits in the grid may be used for storing qubits of a circuit or, as we will see shortly, for routing CNOT gates.

Suppose we wish to execute two parallel CNOT gates. First, we need to choose a logical qubit to encode each of the four qubits in the circuit. This is called a *mapping*. Then, we need to plan the execution of the gates. To execute a CNOT gate on two logical qubits embedded in the same plane, we can use a technique called lattice surgery [17, 22]. A lattice surgery CNOT requires interacting with

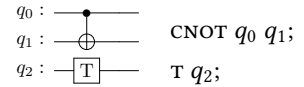


Fig. 1. Two representations of a circuit

an ancilla qubit adjacent to a horizontal boundary of the control qubit (along the top or bottom), and vertical boundary of the target qubit, forming at least one bend. The process of reserving ancillae for gates is called *routing*. In our case, one CNOT gate requires an ancilla connection between  $q_0$  and  $q_3$ , while the other requires one between  $q_1$  and  $q_2$ . As long as these two connections do not overlap, the gates can be performed simultaneously in a single time step. A mapping and routing solution that meets these requirements is shown in Fig. 3. The two routes are indicated by colored squares, with the longer green route corresponding to the CNOT gate applied to  $q_0$  and  $q_1$ .

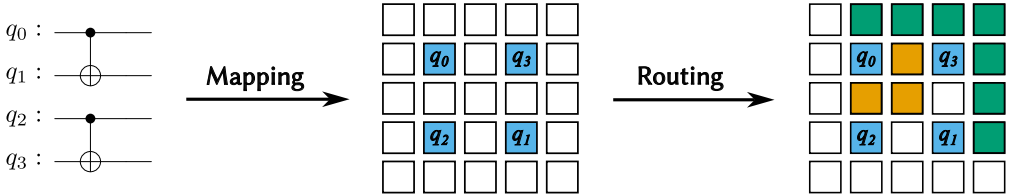


Fig. 3. Simple instance of surface code mapping and routing

We can represent surface code mapping and routing with a grid graph as shown in Fig. 4, which corresponds to the same instance and solution. Specifically, each vertex in the grid represents a logical qubit, and we include an edge between each adjacent pair of logical qubits, not including diagonals.

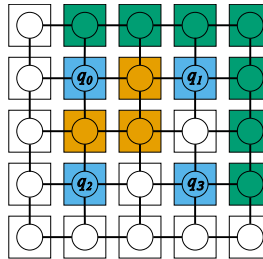


Fig. 4. Representing a surface code mapping and routing problem on a grid graph

**Optimal mapping and routing.** The above example was fairly unconstrained. Any “uniform” mapping leaving an ancilla space between each circuit qubit has a corresponding optimal routing solution. This is not the case in general. Consider the example in Fig. 5 wherein we are mapping the same circuit onto a  $3 \times 3$  subset of our architecture. The depth of this circuit is 1, so it is theoretically executable in a single time step. However, with the choice of the mapping on the left labeled “Mapping 1”, there is no way to simultaneously execute the CNOT gates. Therefore, execution of the circuit will take two time steps. If instead we choose “Mapping 2” on the right, we see there is in fact a routing solution that allows for simultaneous execution, with the routes indicated by colored paths.

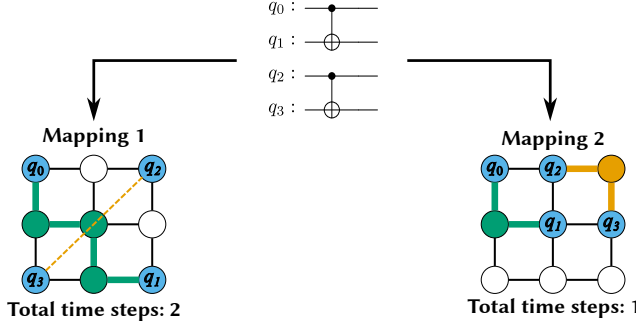


Fig. 5. Example where a suboptimal mapping leads to a longer execution time

**Executing T gates.** The  $T$  gate cannot be applied directly to surface code logical qubits. Instead, executing a  $T$  gate requires applying a lattice surgery CNOT between the input to the  $T$  gate and a logical qubit prepared in a so-called “magic state” [10]. We make a standard assumption that magic state qubits are prepared in a separate region of the plane at a sufficiently high rate such that they are always available at dedicated storage locations. The implication for our mapping and routing problem is that *each T gate must be routed like a CNOT gate with the target qubit chosen from fixed set of vertices provided as part of the input*.

As an example, we return to the circuit in Fig. 1. Since this circuit contains a  $T$  gate, we need to define magic state qubit locations. In Fig. 6, the  $3 \times 3$  architecture has been extended with a column of magic state qubits along the right side, indicated with orange vertices. An optimal mapping and routing solution with one time step is shown. We have two simultaneous connections. One is between qubits  $q_0$  and  $q_1$  and corresponds to the CNOT, while the other is between  $q_2$  and a magic state qubit, corresponding to the  $T$  gate.

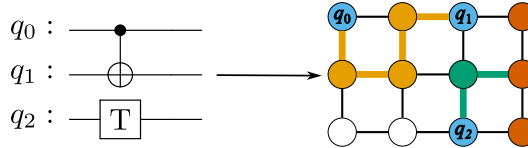


Fig. 6. Example with a  $T$  gate

In summary, the surface code mapping and routing problem consists of two parts:

- (1) **Mapping:** Identify circuit qubits with vertices in a grid graph.
- (2) **Routing:** Assign gates to time steps such that there exist nonoverlapping (vertex-disjoint) paths between the vertices relevant to each gate assigned to a time step.

### 3 THE SURFACE CODE MAPPING AND ROUTING PROBLEM

In this section, we formally define the surface code mapping and routing problem.

**Architectures.** Our abstraction for a fault-tolerant quantum computing architecture is a grid graph with some of the vertices reserved for magic state qubits and others available for storing circuit qubits and routing gates.

We use  $A = (V, E, MS)$  to denote an architecture where

- $G = (V, E)$  is a grid graph and
- $MS \subset V$  are the vertices reserved for magic state qubits.

Formally, we define a grid graph  $G = (V, E)$  to be such that  $V = \{1, \dots, m\} \times \{1, \dots, n\}$  and  $E = \{(v_1, v_2) \in V : \|v_1 - v_2\| = 1\}$ . We say that vertices  $(a, b)$  and  $(c, d)$  are *horizontal neighbors* if  $|a - c| = 1$  and *vertical neighbors* if  $|b - d| = 1$ .

**Qubit maps and valid gate routes.** We will use  $C = \langle g_1, \dots, g_k \rangle$  to denote a circuit represented as a sequence of gate applications. We will sometimes, in a slight abuse of notation, also use  $C$  to denote the underlying set of gate applications that appear in  $C$ .

**DEFINITION 1 (QUBIT MAP).** *Given a circuit  $C$  acting on a set of qubits  $Q$  and an architecture  $A = (V, E, MS)$ , a qubit map is simply an injective function  $M : Q \rightarrow V \setminus MS$ .*

Our goal is to execute a circuit  $C$  as a sequence of time steps. A valid sequence of time steps must respect the logical dependencies in  $C$ . That is, if two gates  $g_i$  and  $g_j$  act on a shared qubit and  $i < j$ , then we say  $g_j$  depends on  $g_i$ , and require that  $g_j$  must be executed after  $g_i$ . Moreover, it must be possible to execute all of the gates assigned to any particular time step simultaneously on the architecture. Gates can be executed simultaneously if there are vertex-disjoint paths, of the proper shape, along which to route them. For CNOT gates, the path must connect the two qubits the CNOT acts on. For T gates, the path must connect a magic state qubit and the qubit the T gate acts on. We say that a function assigning gates to time steps and paths is a *valid gate route* if it meets these requirements. In the definition below,  $\langle V \rangle$  denotes the set of finite sequences of vertices  $\langle v_1, \dots, v_m \rangle$  from a vertex set  $V$ . As with a circuit, we can treat the sequence as a set of elements.

**DEFINITION 2 (VALID GATE ROUTE).** *Given an architecture  $A = (V, E, MS)$ , circuit  $C = \langle g_1, \dots, g_k \rangle$  and qubit map  $M$ , a valid gate route is a value  $t \in \mathbb{N}$  representing a number of time steps, and a pair of functions  $R_{space} : C \rightarrow \langle V \rangle$  and  $R_{time} : C \rightarrow \{1, \dots, t\}$  that meets the following criteria*

- *Data Preservation: No vertex representing a circuit qubit or magic state qubit is used for routing. That is, for any vertex  $v \in M(Q) \cup MS$ ,  $v$  can only appear in either the first or last position of a sequence in the image of  $R_{space}$ .*
- *CNOT Routing: If  $g = \text{CNOT } q_i \text{ } q_j$ , then  $R_{space}(g)$  is a path  $\langle M(q_i), v_1, \dots, v_{n-1}, M(q_j) \rangle$  where  $v_1$  is a vertical neighbor of  $M(q_i)$  and  $v_{n-1}$  is a horizontal neighbor of  $M(q_j)$ .*
- *T Routing: If  $g = T \text{ } q_i$ , then  $R_{space}(g)$  is a path  $\langle M(q_i), v_1, \dots, v_{n-1}, v_n \rangle$  where  $v_n \in MS$ ,  $v_1$  is a vertical neighbor of  $M(q_i)$ , and  $v_{n-1}$  is a horizontal neighbor of  $v_n$ .*
- *Logical Order: If  $i < j$ ,  $g_i$  and  $g_j$  act on the same qubit, then  $R_{time}(g_i) < R_{time}(g_j)$ .*
- *Disjoint Paths: If  $R_{time}(g_i) = R_{time}(g_j)$ ,  $R_{space}(g_i) \cap R_{space}(g_j) = \emptyset$ .*

With this terminology in place, the surface code mapping and routing problem can be concisely defined as the task of finding a qubit map and gate route pair with the minimal number of time steps.

**DEFINITION 3 (SURFACE CODE MAPPING AND ROUTING PROBLEM).**

*Given: An architecture  $A$  and a circuit  $C$ .*

*Find: A qubit map  $M$  and a valid gate route  $(t, R_{time}, R_{space})$  for  $A, C$  and  $M$  such that  $t$  is minimized.*

We will abbreviate “Surface Code Mapping and Routing Problem” as SCMR and denote an instance with architecture  $A$  and circuit  $C$  by  $\text{SCMR}(A, C)$ .

#### 4 HARDNESS OF SURFACE CODE COMPIILATION

In this section, we prove that surface code mapping and routing is NP-complete via a reduction from a multiprocessor scheduling problem. To that end, we state the decision version of the SCMR problem below.

**DEFINITION 4 (SCMR DECISION PROBLEM).**

*Given: An architecture  $A$  and circuit  $C$  and time limit  $t_s$*

*Question: Is there a qubit map  $M$  and valid gate route  $(t, R_{\text{space}}, R_{\text{time}})$  for  $A, C$ , and  $M$  with  $t \leq t_s$ ?*

**THEOREM 4.1.** *The scmr Decision Problem is NP-complete.*

#### 4.1 The Routing Problem is NP-Complete

We open with the observation that the surface code routing problem is NP-complete even for a given fixed map.

**DEFINITION 5 (SURFACE CODE ROUTING DECISION PROBLEM).**

*Given: An architecture  $A$  and circuit  $C$ , a qubit map  $M$ , and time limit  $t_s$*

*Question: Is there a valid gate route  $(t, R_{\text{space}}, R_{\text{time}})$  for  $A, C, M$  with  $t \leq t_s$ ?*

**THEOREM 4.2.** *The Surface Code Routing Decision Problem is NP-complete.*

Consistent with notation from Section 3, we denote the surface code routing instance with architecture  $A$ , circuit  $C$ , and qubit map  $M$  by  $\text{SCR}(A, C, M)$ . Clearly  $\text{SCR}$  is in NP, with a sequence of time steps representing a valid gate route serving as a polynomial length certificate. We prove the hardness part of Theorem 4.2 by noting  $\text{SCR}$  is closely related to an NP-complete problem originally considered in the context of VLSI layout [29].

**DEFINITION 6 (NODE-DISJOINT PATHS ON A GRID PROBLEM).**

*Given: A grid graph  $G = (V, E)$  and a set of vertex pairs  $\mathcal{R} = \{(s_1, t_1), \dots, (s_k, t_k)\}$*

*Question: Do there exist vertex-disjoint paths connecting  $s_i$  to  $t_i$  for each pair  $(s_i, t_i) \in \mathcal{R}$ ?*

Node-Disjoint Paths on a Grid can be reduced to Surface Code Routing because the former problem is essentially just the special case of the latter where there are no dependencies and one time step. The only complication is that not every set of disjoint paths is a valid gate route because of the additional requirement that paths must terminate in a vertical edge at the control qubit and a horizontal edge at the target. See Appendix A for our construction which resolves this issue.

#### 4.2 Overview of the Proof of Theorem 4.1

Once again  $\text{SCMR}$  is in NP, with a polynomial length certificate consisting of a description of the qubit map and a sequence of time steps representing a valid gate route (alternatively, our poly-sized SAT encoding in Section 5 is a constructive proof). The hardness proof is a reduction from the k-processor scheduling problem, shown to be NP-complete by Ullman [45] and stated below.

**DEFINITION 7 (PROCESSOR SCHEDULING PROBLEM).**

*Given: a finite partially ordered set of jobs  $(J, \prec)$ , a number of processors  $k$ , and a time limit  $t_p$*

*Question: Does there exist a schedule  $s$  from  $J$  to the set  $\{1, \dots, t_p\}$  such that*

- if  $j \prec j'$  then  $s(j) < s(j')$ ;
- for each  $1 \leq i \leq t_p$ , the subset of  $J$  mapped to  $i$  by  $s$  has cardinality at most  $k$ ?

We will abbreviate ‘Processor Scheduling Problem’ as PSP and denote an instance with a job set  $(J, \prec)$ ,  $k$  processors, and time limit  $t_p$  by  $\text{PSP}(J, k, t_p)$  (leaving the order implied). PSP is a natural choice for this reduction since it also involves executing tasks with dependencies as a sequence of time steps, but without the space constraints of  $\text{SCMR}$ . Just as a job occupies a processor for a time step, a T gate occupies a magic state qubit for a time step. Therefore the overall strategy of the proof is to encode the dependency structure of a PSP instance into the T gates of a circuit, and include the same number of magic state qubits as processors to match the simultaneous capacity.

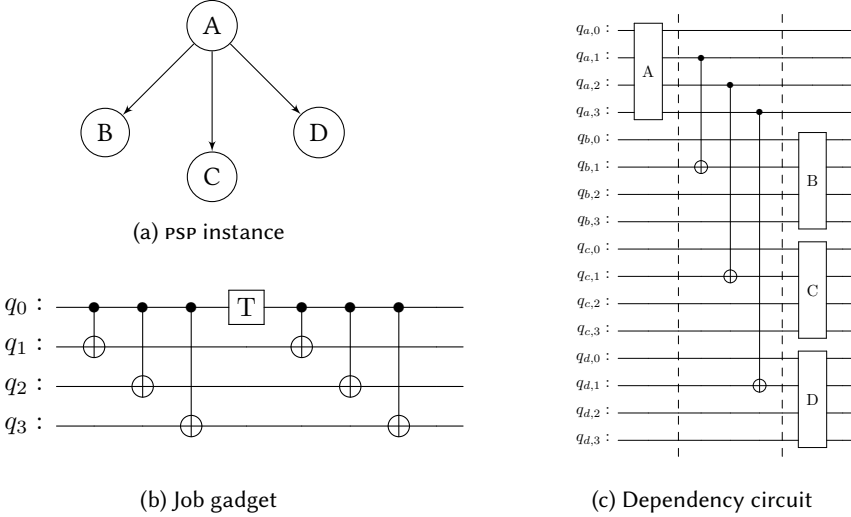


Fig. 7. Constructing the dependency circuit for our running example. Each rectangle in the dependency circuit shown in (c) is one copy of the circuit in (b)

We will walk through this process with the example job set shown in Fig. 7a. For the full proof see Appendix B. This instance consists of four jobs: one has no prerequisites and the other three depend solely on it. Our goal is the following:

*Associate each job in a PSP instance with a T gate, such that the dependency structure of the resulting circuit is exactly that of the PSP instance.*

There are three roadblocks along this path which motivate the three major components of the reduction.

*Challenge 1 (High-degree jobs):* Since quantum gates act on at most two qubits, we cannot directly encode jobs with more than two dependencies, such as Job A in our example set.

*Solution:* Represent each job with a subcircuit called a job gadget containing exactly one T gate and several CNOT gates. The job gadget representing the jobs in our example is shown in Fig. 7b. The T gate of the job gadget is applied to the first qubit. The other qubits are used to induce dependencies between T gates. In our example, the maximum number of incoming or outgoing dependencies for a job is three, so we have three of these additional “input/output” (I/O) qubits. Notice that if we construct a circuit where a job gadget is preceded by a gate  $g$  on one of its I/O qubits, then the T gate depends on  $g$  transitively via one of the first three CNOT gates in the job gadget. Likewise, in a circuit where a job gadget is followed by a gate  $g$  on one of its I/O qubits,  $g$  depends on the T gate through one of the last three CNOT gates in the job gadget. We use this property of the job gadget to induce the appropriate dependencies between job gadgets in a *dependency circuit*. In the dependency circuit, we include a CNOT between I/O qubits of job gadgets for each direct dependency of jobs. Parallel dependencies (like A to B and A to C in our example) use different I/O qubits. The full dependency circuit corresponding to this example is in Fig. 7c.

*Challenge 2 (Time Dilation):* We need a longer time limit for our SCMR instance than the original PSP instance. Consider the instance consisting of our running job set,  $k = 3$  processors, and the time limit  $t_p = 2$ . Clearly, the answer is “yes”: execute job A in step 1 and the other three jobs in

step 2. Two steps is not sufficient for executing the dependency circuit because we have “stretched” each job into several gates and added “transition” CNOT gates between job gadgets.

*Solution:* Choose an extended time limit for the SCMR instance with both a stretching and transition term. In our case, each job gadget includes a chain of 7 dependent gates, so the stretching term is  $7t_p$ . Since the maximum number of dependencies of a job is 3 and we have  $k$  independent processors, we need to be able to execute up to  $3k$  transition CNOT gates between jobs. This yields a transition term of  $3k(t_p - 1)$ , for a total time limit of  $t_s = 7t_p + 3k(t_p - 1)$ .

*Challenge 3 (Staggered Execution):* When we choose a time limit that accounts for the stretching and transitions, we over-correct and introduce spurious solutions. Using the same set of jobs and time limit of  $t_p = 2$ , the answer is “no” with only  $k = 2$  processors. The formula in the previous paragraph yields  $t_s = 20$  time steps to execute the dependency circuit. The dependency circuit *can* be executed within 20 steps, even with a magic state capacity limit of 2. This can be done by delaying the execution of job gadget D by one time step. Then, only two T gates are executed simultaneously (for B and C), and the job set is executed in 18 total steps. Such a solution breaks the correspondence between PSP and SCMR.

*Solution:* Eliminate the unwanted solutions by adding an independent circuit called the *cycle circuit*. The cycle circuit applies  $t_s$  gates to each qubit, so it can be executed in  $t_s$  steps only when each gate is executed as soon as theoretically possible, at the time step equal to its depth in the circuit. This is useful because it allows us to restrict the execution of T gates in the dependency circuit to specific time steps. The cycle circuit occupies and releases the magic state qubits in a repeating cycle. The number of cycles is equal to the PSP time limit  $t_p$ . The T gates from the dependency circuit are executable only in the steps that lie at the center of a cycle (where the cycle circuit executes a CNOT), and there are  $t_p$  such steps. Now, it is no longer possible to delay the execution of job gadget D by one time step because no magic state qubits are available.

Fig. 8 shows the dependency circuit extended with the cycle circuit. One pair of qubits is shown, corresponding to a PSP instance with a single processor. To encode  $k$  processors, we include  $k$  copies of the two-qubit circuit.

*The architecture.* Since the T gates in the dependency circuit correspond to jobs, we design our target architecture to match the capacity of a PSP instance with  $k$  processors by including  $k$  magic state qubits, so that  $k$  T gates can be executed simultaneously. Other than this capacity limit, we do not want to introduce any additional limitations. If two jobs can be assigned to the different processors at the same time step, their job gadgets should be simultaneously executable. We ensure this property by organizing our architecture into  $k$  “processor units.” Each processor unit contains one magic state qubit. We can connect processor units into a connected grid arbitrarily. For simplicity, we choose to chain them linearly, forming a “long” architecture with 4 rows and many columns.

*Summary.* Given a PSP instance  $(J, k, t_p)$ , we can construct an equivalent SCMR instance  $(A, C, t_s)$  where  $A$  consists of  $k$  processor units,  $C$  is the union of the dependency circuit and the cycle circuit, and  $t_s$  is computed as described above from the number of processors and the maximum number of dependencies of a job. We can translate solutions from one instance to another by executing a job in step  $i$  on processor  $j$  if and only if the corresponding job gadget is executed during cycle  $i$  of the cycle circuit and the job circuit qubits are mapped to processor unit  $j$ . See Appendix B for a detailed proof.

## 5 OPTIMAL SURFACE CODE MAPPING AND ROUTING ALGORITHM

We now describe our encoding of an SCMR decision problem instance into SAT which is the basis of our optimal algorithm. Throughout we will fix an architecture  $A = (V, E, MS)$ , a circuit  $C =$

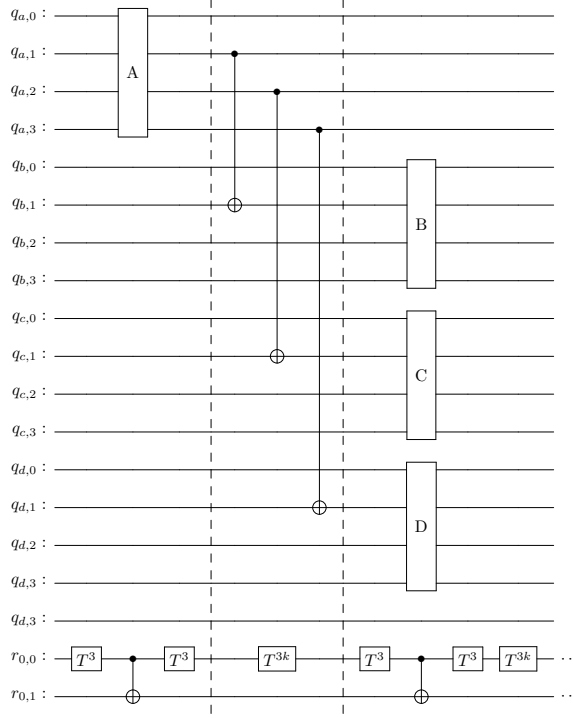


Fig. 8. Full circuit in our reduction. The notation  $T^x$  means  $x$  applications of the  $\tau$  gate

$\langle g_1, \dots, g_k \rangle$  acting on qubits in a set  $Q$  and a time limit  $t_s$ . Our encoding includes three types of boolean variables: the map variables represent the qubit mapping, the exec variables represent the assignment of gates to time steps (the function  $R_{time}$ ) and the path variables represent the path used to route gates (the function  $R_{space}$ ). The formula over these variables that we produce will enforce that the qubit map encoded by map and the routing encoded by exec and path are a valid solution as defined in Section 3. In describing these constraints, we use cardinality constraints which enforce that *at most one* (AMO) or *exactly one* (EO) of a set of variables is set to true. The efficient translation of cardinality constraints into conjunctive normal form is a well-studied area [5, 7, 19, 36, 39] so we leave the encoding unspecified for simplicity.

**Variables.** The boolean variables that appear in our encoding are listed below along with their intended semantics.

- $\text{map}(q, v)$ : the qubit  $q$  in the circuit is mapped to the vertex  $v$ .
- $\text{exec}(g, t)$ : the gate  $g$  is executed in time step  $t$ .
- $\text{path}(u, v, g, t)$ : the edge  $(u, v)$  is used in the path for gate  $g$  at time step  $t$ .

## 5.1 Constraints

**Maps are injective functions.** To enforce that a satisfying assignment corresponds to a valid qubit map, we require that for each  $q$  there is *exactly one*  $v$  where  $\text{map}(q, v)$  is set to true (functional consistency) and that for each  $v$  there is *at most one*  $q$  where  $\text{map}(q, v)$  is set to true (injectivity).

These constraints are shown below.

$$\text{MAP-VALID} \triangleq \bigwedge_{q \in Q} \text{EO}(\{\text{map}(q, v) : v \in V \setminus MS\}) \wedge \bigwedge_{v \in V \setminus MS} \text{AMO}(\{\text{map}(q, v) : q \in Q\})$$

**Paths preserve data.** We cannot overwrite circuit qubits or magic state qubits in the routing process. In terms of path and map variables, this means that we cannot set both  $\text{path}(u, v, g, t)$  and  $\text{path}(v, w, g, t)$  for any  $u, w, g$ , and  $t$  if we have set  $\text{map}(q, v)$  for some qubit  $q$  or if  $v \in MS$ .

$$\begin{aligned} \text{CIRC-SAFE} &\triangleq \bigwedge_{\substack{u, v, w \in V \\ t \leq t_s \\ q \in Q, g \in C}} \neg \text{map}(q, v) \vee \neg \text{path}(u, v, g, t) \vee \neg \text{path}(v, w, g, t) \\ \text{MS-SAFE} &\triangleq \bigwedge_{\substack{v \in MS, u, w \in V \\ t \leq t_s \\ g \in C}} \neg \text{path}(u, v, g, t) \vee \neg \text{path}(v, w, g, t) \\ \text{DATA-SAFE} &\triangleq \text{CIRC-SAFE} \wedge \text{MS-SAFE} \end{aligned}$$

**All gates are executed in logical order.** To ensure that all gates are executed in a valid order, we enforce that for each  $g$ , there is exactly one  $t$  such that  $\text{exec}(g, t)$  is set to true and that if  $g_j$  depends on  $g_i$ , (which we denote with  $g_i \prec g_j$ ), then  $\text{exec}(g_i, t)$  implies  $\text{exec}(g_j, t')$  for some  $t' > t$ . This is represented by the constraints:

$$\text{GATES-ORDERED} \triangleq \bigwedge_{g \in C} \text{EO}(\{\text{exec}(g, t) : t \leq t_s\}) \wedge \bigwedge_{\substack{g \prec g' \\ t' \leq t}} \neg \text{exec}(g, t) \vee \neg \text{exec}(g', t')$$

**Paths are disjoint.** Though the edges in the underlying graph are undirected, it is useful for our formulation to assign a direction to the paths, so we assign the direction of the edge as from  $u$  to  $v$  if  $\text{path}(u, v, g, t)$  is set to true. We require that our simultaneous paths are *vertex* disjoint, meaning each vertex can have at most one incoming edge and at most one outgoing edge. Therefore, for each time step  $t$  and vertex  $u$ , we include the constraint that there is at most one pair  $v, g$  such that  $\text{path}(u, v, g, t)$  is set to true and at most one pair  $v', g'$  such that  $\text{path}(v', u, g', t)$  is set to true<sup>1</sup>:

$$\text{DISJOINT} \triangleq \bigwedge_{\substack{t \leq t_s \\ u \in V}} \text{AMO}(\{\text{path}(u, v, g, t) : v \in V, g \in C\}) \wedge \text{AMO}(\{\text{path}(v', u, g', t) : v' \in V, g' \in C\})$$

**Paths connect CNOT pairs.** The most complicated type of constraints are those that enforce that the path variables encode a valid path between the relevant vertices. We start with the case of CNOT gates. The constraints effectively construct a path inductively. Let  $g = \text{CNOT } q_i \, q_j$  be a CNOT gate. The path corresponding to  $g$  must begin at a vertical neighbor of the control qubit  $q_i$  and terminate at a horizontal neighbor of the target qubit  $q_j$ . This leads to the “base case” constraint for each vertex. If  $\text{map}(q_i, v)$  and  $\text{exec}(g, t)$  are both set to true, then there is a vertical neighbor of  $v$  such that  $\text{path}(v, u, g, t)$  is set to true. Likewise, if  $\text{map}(q_j, v)$  and  $\text{exec}(g, t)$  are both set to true, then there is a horizontal neighbor of  $v$  such that  $\text{path}(u, v, g, t)$  is set to true. We state this below using

<sup>1</sup>In fact,  $g'$  must be equal to  $g$  but this is implied by the remaining constraints.

$VN(v)$  (and  $HN(v)$ ) as an abbreviation for the set of up to two vertical (and horizontal) neighbors of a vertex  $v$ :

$$\begin{aligned} \text{CNOT-START} &\triangleq \bigwedge_{\substack{v \in V \\ g(q_i, q_j) \in C \\ t \leq t_s}} \left( \neg \text{map}(q_i, v) \vee \neg \text{exec}(g, t) \vee \bigvee_{u \in VN(v)} \text{path}(v, u, g, t) \right) \\ \text{CNOT-REACH-TARGET} &\triangleq \bigwedge_{\substack{v \in V \\ g(q_i, q_j) \in C \\ t \leq t_s}} \left( \neg \text{map}(q_j, v) \vee \neg \text{exec}(g, t) \vee \bigvee_{u \in HN(v)} \text{path}(u, v, g, t) \right) \end{aligned}$$

Then, the inductive step is the constraint that for each edge  $(u, v)$  on the path, either  $u$  is a valid starting point for the path, or an internal vertex on the path. In the latter case, it must be incident to another edge to follow back towards the starting point. In our variables, we can express the two options as  $\text{path}(u, v, g, t)$  implies either  $\text{path}(w, u, g, t)$  for some distinct vertex  $w$  adjacent to  $u$  or  $\text{map}(q_i, u)$ .

$$\text{CNOT-INDUCTIVE} \triangleq \bigwedge_{\substack{g(q_i, q_j) \in C \\ t \leq t_s \\ (u, v) \in E}} \left( \neg \text{path}(u, v, g, t) \vee \bigvee_{\substack{(w, u) \in E \\ w \neq v}} \text{path}(w, u, g, t) \vee \text{map}(q_i, u) \right)$$

$$\text{CNOT-ROUTED} \triangleq \text{CNOT-START} \wedge \text{CNOT-REACH-TARGET} \wedge \text{CNOT-INDUCTIVE}$$

**Paths connect T targets to magic states.** Let  $g = \tau q_j$  be a T gate. We also need to enforce that the path variables assign an appropriate path between  $q_j$  and a magic state qubit. This type of constraint is similar to the previous. The only difference is in the definition of valid end points which are now horizontal neighbors of magic state qubits.

$$\text{T-REACH-TARGET} \triangleq \bigwedge_{\substack{g(q) \in C \\ t \leq t_s}} (\text{EO}(\{\text{path}(u, v, g, t) : v \in MS, u \in HN(v)\}))$$

$$\text{T-ROUTED} \triangleq \text{T-START} \wedge \text{T-REACH-TARGET} \wedge \text{T-INDUCTIVE}$$

The full formula corresponding to an SCMR instance is given by the conjunction of all of these constraints:

$$\varphi(A, C, t_s) \triangleq \text{MAP-VALID} \wedge \text{GATES-ORDERED} \wedge \text{DATA-SAFE} \wedge \text{DISJOINT} \wedge \text{CNOT-ROUTED} \wedge \text{T-ROUTED}$$

**THEOREM 5.1.** *The formula  $\varphi(A, C, t_s)$  is satisfiable if and only if the answer to the decision problem  $\text{SCMR}(A, C, t_s)$  is “yes” and there is an explicit translation from solutions to  $\text{SCMR}(A, C, t_s)$  to models of  $\varphi(A, C, t_s)$  and vice-versa.*

Theorem 5.1 implies a natural optimal algorithm for solving SCMR with a SAT oracle by initializing  $t_s$  to the depth of  $C$ , querying the satisfiability of  $\varphi(A, C, t_s)$ , incrementing  $t_s$  if the result is “unsatisfiable,” and repeating until a solution is found. We call this algorithm OPTIMAL.

## 6 RELAXATIONS: MAPPING STRATEGIES AND GREEDY ROUTING

While OPTIMAL guarantees the best SCMR solution, the SAT-solving subroutine is infeasible to apply to large circuits, motivating the development of more efficient techniques that sacrifice optimality. Our approach is to decouple the subproblems of mapping and routing and solve them separately.

## 6.1 Routing

**Greedy Routing.** We begin by describing GREEDY-ROUTE, a greedy algorithm with a known approximation ratio for the routing problem. GREEDY-ROUTE considers only one time step at a time, attempting to execute as many gates as possible simultaneously. Unfortunately, as noted in Section 4.1, determining whether a set of parallel gates can be routed simultaneously is essentially the NP-complete Node-Disjoint Paths problem (Definition 6), which asks whether vertex-disjoint paths exist between all pairs of vertices in a given set. Our goal of routing as many gates as possible is therefore equivalent to the *optimization version* of NDP, which asks for the maximum-size subset of the given pairs for which there are vertex-disjoint paths.

This leads to another instance of greediness, where we leverage existing work and apply a well-known greedy algorithm [28] for approximating the optimization version of NDP. The algorithm is simple: while there is a path along which to route a logically executable gate, choose the shortest such path to add to the current time step, and delete the vertices from the underlying graph. We refer to this greedy algorithm for NDP as SHORTEST-FIRST (see Algorithm 1). The guarantee of SHORTEST-FIRST is that it connects  $O(\sqrt{n} \cdot OPT)$  pairs of vertices where  $OPT$  is the number of pairs connected by the optimal solution and  $n$  is the number of vertices in the graph.

---

**Algorithm 1** Shortest-First NDP Algorithm

---

```

1: procedure SHORTEST-FIRST(graph  $G$ , vertex pairs  $\mathcal{R}$ )
2:    $step \leftarrow \emptyset$ 
3:   while there exists a pair in  $\mathcal{R}$  that can be routed by a path in  $G$  do
4:     Let  $(s, t)$  be the pair in  $\mathcal{R}$  with minimum shortest-path length
5:     Let  $p$  be a shortest path from  $s$  to  $t$ 
6:      $step \leftarrow step \cup \{p\}$ 
7:     Remove all vertices in  $p$  from  $G$ 
8:   return  $step$ 

```

---

The GREEDY-ROUTE algorithm is shown in full in Algorithm 2. To build sets of parallel gates, we partition a circuit with depth  $d$  into  $d$  sets of gates called topological layers  $l_1, \dots, l_d$ , such that if  $g'$  depends on  $g$  in layer  $l_i$ , then  $g'$  appears in a later layer  $l_{i+k}$  with  $k \geq 0$ . Then a circuit can be routed layer-by-layer. For a given layer, we repeatedly apply SHORTEST-FIRST, greedily routing subsets of the layer until all gates have been routed.

---

**Algorithm 2** Greedy Routing Algorithm

---

```

1: procedure GREEDY-ROUTE(architecture  $A = (G, MS)$ , circuit  $C$ , map  $M$ )
2:   Let  $l_1, \dots, l_d$  be a topological layering of  $C$ 
3:    $steps \leftarrow \langle \rangle$ 
4:   for each layer  $l_i$  do
5:     Let  $unrouted$  be the pairs of vertices in  $G$  to be routed for the gates in  $l_i$  under the map  $M$ 
6:     while  $unrouted \neq \emptyset$  do
7:        $next \leftarrow \text{SHORTEST-FIRST}(G, unrouted)$ 
8:        $steps.append(next)$ 
9:       Remove each pair routed in  $next$  from  $unrouted$ 
10:  return  $steps$ 

```

---

We can derive an approximation ratio for GREEDY-ROUTE based on the known  $O(\sqrt{n})$ -approximation ratio for SHORTEST-FIRST and a technique from prior work that uses this approximation ratio to bound the number of applications of SHORTEST-FIRST [6, 8].

**THEOREM 6.1.** *GREEDY-ROUTE( $A, C, M$ ) is an  $O(d\sqrt{n} \log q)$ -approximation algorithm for surface code routing where  $n$  is the number of vertices in  $A$ ,  $q$  is the number of qubits in  $C$ , and  $d$  is its depth.*

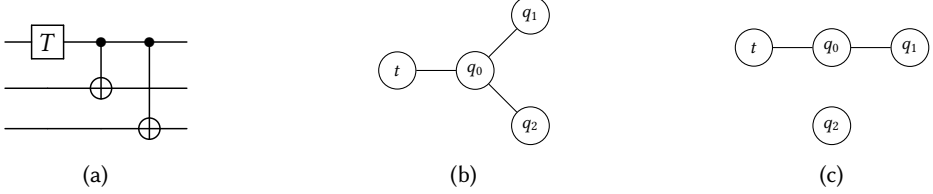


Fig. 9. Circuit with corresponding interaction graph (b) and interaction chain set (c)

## 6.2 Mapping

The remaining piece to construct a full algorithm for SCMR is a mapping algorithm to construct the input for the routing algorithm. Each composition of mapping and routing yields a unique SCMR algorithm. Thus, for each mapping strategy we obtain two new SCMR algorithms: one by composition with GREEDY-ROUTE and one by composition with optimal routing (applying OPTIMAL with constraints enforcing a fixed input map). We present two different mapping algorithms: a randomized method and one based on the simple heuristic of placing interacting qubits close to one another.

**Randomized Mapping.** The simplest approach is to make no attempt to optimize the qubit map at all, sampling uniformly at random from the set of possible maps. This is the extreme end of prioritizing run time over solution quality. We can find better solutions at a linear computational cost by sampling more than one random map, applying the routing algorithm to each, and returning the best result. We call this algorithm RAND-MAP-N where  $N$  is the number of maps in the random sample.

**Structural Mapping.** Alternatively, one could analyze the input circuit in order to select a compatible qubit map. One useful heuristic is that shorter routes are less likely to conflict with others because they occupy fewer vertices. Therefore, it is advantageous to map interacting qubits near one another to allow for more short gate routes. This is the principle which guides STRUCT-MAP, our other linear-time mapping algorithm. We can express the qubit interactions of a circuit  $C$  via its *interaction graph*  $I_C$ . The graph  $I_C$  has a vertex for each qubit and an undirected edge  $(q_i, q_j)$  for each pair such that CNOT  $q_i q_j$  is a gate in  $C$ . To account for interactions with magic states, we include an additional vertex  $t$  and an edge  $(t, q_i)$  for each  $q_i$  such that  $\text{T } q_i$  appears in  $C$ . See Fig. 9a and Fig. 9b for an example of a circuit and its interaction graph.

Ideally, we would like a qubit map  $M$  such that for every edge  $(q_i, q_j)$  in  $I_C$  the distance between  $M(q_i)$  and  $M(q_j)$  is small, and every qubit adjacent to  $t$  in  $I_C$  is mapped near a magic state qubit. However, it is not clear how to construct such a map efficiently. Instead we consider an under-approximation of  $I_C$ , inspired by techniques for the CNOT routing problem in the setting of near-term quantum computers without error-correction [15]. Namely, we decompose  $I_C$  into an *interaction chain set*. An interaction chain set is a set of maximal paths in  $I_C$  such that no qubit vertex appears in multiple paths, and each path includes at most one edge incident to  $t$ . As its name suggests, the paths in an interaction chain set can be viewed as “chains” of interacting qubits. Each link in the chain represents one or more CNOT gates in the circuit that will have a short path length if adjacent qubits in the chain are placed in adjacent locations. Fig. 9c shows an interaction chain set derived from the interaction graph in Fig. 9b:  $\langle t, q_0, q_1 \rangle$  and  $\langle q_2 \rangle$ . Notice that we have dropped the interaction between  $q_0$  and  $q_2$  because  $q_0$  cannot be included in both chains.

STRUCT-MAP (Algorithm 3) constructs an interaction chain set, then chooses a qubit map according to its edges in one linear pass, placing the chains on the architecture one at a time. To place a chain, it applies the following subroutine (MAP-CHAIN). If a chain includes the vertex  $t$ , it starts from

this end, placing the qubit adjacent to  $t$  in the chain nearly adjacent to a magic state qubit on the architecture, leaving one vertex between each qubit to facilitate the bend in the path. Otherwise it chooses an end and places the first qubit arbitrarily. From here, the qubits of the chains are laid out on the architecture in order. Each qubit is mapped nearly adjacent to the previous, again leaving one vertex between each to facilitate the bend in the path. If at any point the algorithm gets “stuck” with no choice for the next qubit, it chooses a free vertex arbitrarily (see line 17). Theorem 6.2 establishes the correctness and runtime of STRUCT-MAP.

---

**Algorithm 3** Structural Mapping Algorithm
 

---

```

1: procedure STRUCT-MAP(architecture  $A = (V, E, MS)$ , circuit  $C$ )
2:   Let  $\mathcal{P}$  be an interaction chain set for  $C$ .
3:    $available \leftarrow V \setminus MS$ 
4:   return  $\bigcup_{P \in \mathcal{P}} \text{MAP-CHAIN}(P)$ 
5: procedure MAP-CHAIN( $P$ )
6:    $M \leftarrow \emptyset$ 
7:   Assign a direction to  $P$  such if  $t \in P$ , it is the last vertex.
8:   if  $P = \langle t \rangle$  then ▷ base case for chains including  $t$ 
9:     return  $M$ 
10:  else if  $P$  is a single vertex  $q \neq t$  then ▷ base case for chains not including  $t$ 
11:     $M(q) \leftarrow available.pop()$ 
12:    return  $M$ 
13:  else
14:     $q, P' \leftarrow head(P), tail(P)$ 
15:     $M \leftarrow M \cup \text{MAP-CHAIN}(P')$ 
16:    Let  $neighbors$  be the subset of  $available$  with distance 2 from  $M(head(P'))$  ▷ With the convention  $M(t) = MS$ 
17:     $M(q) \leftarrow neighbors.pop()$  if  $neighbors \neq \emptyset$  else  $available.pop()$ 
18:    Remove  $M(q)$  from  $available$  if not removed in previous step
19:  return  $M$ 
  
```

---

**THEOREM 6.2.** *Given an architecture  $A$  and circuit  $C$ , STRUCT-MAP terminates in linear time (in the size of  $A$  and  $C$ ) and returns a qubit map.*

## 7 KNOWN-OPTIMAL CIRCUITS

In evaluating the performance of our algorithms, it is useful to know the value of the optimal solution. To this end, we develop a simple procedure for generating nontrivial circuits that can be executed with zero overhead, i.e. in a number of time steps equal to the depth. For any nonnegative integers  $k$  and  $d$ , to generate a circuit with an optimal solution using  $d$  time steps on  $2k$  qubits, we choose a random even partition of the qubits into two ordered lists (of size  $k$ ). Let LEFT and RIGHT denote these lists. The circuit then consists of  $d$  CNOT gates between LEFT[i] and RIGHT[i] for  $1 \leq i \leq k$ . For example, if we instantiate this procedure with  $d = 2$  and  $k = 3$ , one possible outcome is the circuit in Fig. 10a. This corresponds to the partition LEFT =  $\langle 0, 1, 5 \rangle$ , RIGHT =  $\langle 2, 3, 4 \rangle$ . We use KNOWN-OPTIMAL( $d, k$ ) to denote this circuit generation algorithm with parameters  $d$  and  $k$ .

**THEOREM 7.1.** *KNOWN-OPTIMAL( $d, k$ ) produces a circuit  $C$  for which the problem SCMR( $A, C$ ) has optimal value  $d$  for any architecture  $A$  with a  $2\lceil\sqrt{k}\rceil \times 2\lceil\sqrt{k}\rceil$  subgrid with no magic state vertices.*

The intuition is that each qubit has a unique “partner,” (adjacent qubit in the interaction graph) so all logically parallel CNOT gates can be performed simultaneously by dedicating a  $2 \times 2$  square to each pair of interacting qubits. Under such a mapping, the gates be routed entirely within the corresponding square, avoiding any crossing of paths. Therefore, the optimal solution is equal to the theoretical lower bound of the circuit depth.

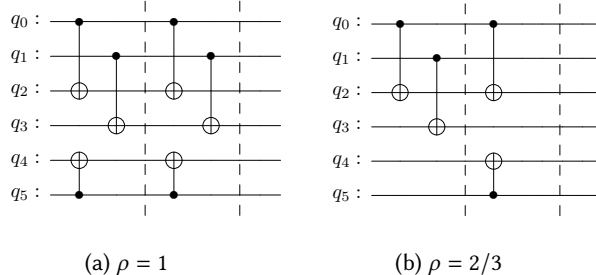


Fig. 10. Two synthetic circuits produced by the KNOWN-OPTIMAL procedure

Notice that we can reduce the number of gates without affecting the depth by omitting some of the CNOT gates. We extend the procedure above to take a parameter called the *density*  $\rho \in (0, 1]$  such that, in each iteration,  $\lceil \rho \cdot k \rceil$  of the  $k$  possible CNOT gates are included in the circuit. The circuit from Fig. 10a has a density of  $\rho = 1$ . Suppose instead we choose a density of  $\rho = 2/3$  with  $d = 2$  and  $k = 3$  as before. Then the partition  $\text{LEFT} = \langle 0, 1, 5 \rangle$ ,  $\text{RIGHT} = \langle 2, 3, 4 \rangle$  now corresponds to the circuit in Fig. 10b, with one CNOT gate omitted per layer.

## 8 IMPLEMENTATION AND EVALUATION

**Implementation.** We implemented the SCMR algorithms presented in Section 5 and Section 6 to perform an empirical evaluation. The implementation of OPTIMAL generates the constraints, then queries the SAT solver CaDiCal [9] via the PySAT toolkit [24].

**Research questions.** Our experimental evaluation is designed to answer the following research questions:

- (RQ1) How does the compilation time scale with problem size?
- (RQ2) How close to optimal are the solutions of relaxations?
- (RQ3) What is the effect of varying magic state placement?

**Benchmarks.** Our evaluation is performed on a benchmark suite consisting of both quantum application circuits and synthetic circuits. We collected 169 application circuits. Some of these are implementations of full quantum algorithms: Shor’s Algorithm, the Quantum Fourier Transform, and Grover’s Algorithm. Others are common arithmetic subroutines from the RevLib [48] suite. The synthetic circuits are designed to provide further insight into the generic performance of our techniques. Specifically we will consider the known-optimal circuits described in Section 7 as well as randomly generated circuits.

**Experimental setup.** In this evaluation, we focus on architectures with a regular structure. This means that we restrict the qubit map such that each qubit in the circuit is at the center of a  $3 \times 3$  subgrid that contains no other mapped qubits, see the map in Fig. 3 as an example. This matches the regular structure assumed in prior work [8, 22]. The advantage of this assumption is that every circuit is eventually executable under every mapping, in the worst case requiring one time step per gate. We choose the smallest architecture for which these mappings exist. Since each possible mapping location must be adjacent to two empty rows and columns, this amounts to a  $(2\lceil\sqrt{n}\rceil + 1) \times (2\lceil\sqrt{n}\rceil + 1)$  region, where  $n$  is the number of qubits in the circuit. Except in addressing (RQ3), we assume this region is surrounded with magic state qubits on all sides. Each tool was allotted a 1hr timeout per circuit and 32GB of RAM on a cluster of Intel® Xeon® and AMD Opteron™ CPUs clocked an average of 2.5GHz.

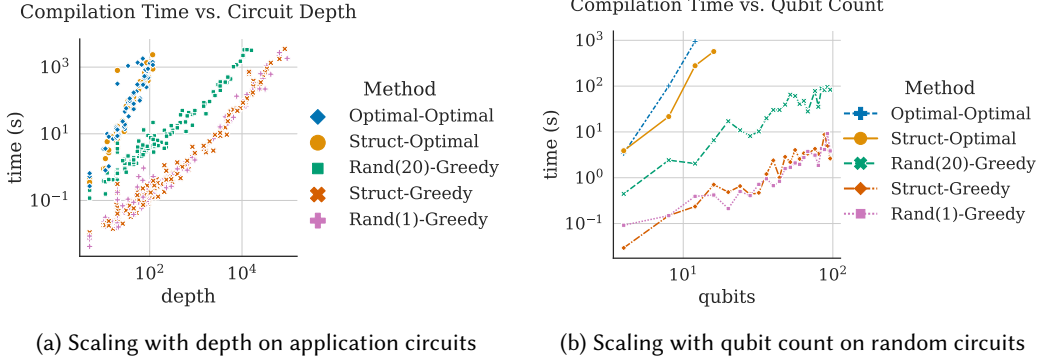


Fig. 11. Compilation time as a function of problem size

### (RQ1): How does the compilation time scale with problem size?

*Summary: Solving the optimal encoding is infeasible with more than a few qubits and a depth beyond about 100. All of the relaxations are significantly more scalable, solving instances with depth in the tens of thousands within the 1hr timeout.*

We explore problem size in two dimensions by scaling both the depth and the qubit count.

**Depth.** Fig. 11a shows the runtime of different methods on the applications circuits. The x-axis of the plot represents the depth of the circuit. Since the depth is a lower bound on the number of steps required to execute a circuit, this can be thought of as the complexity of problem instance in the “time” dimension. The y-axis represents the compilation time (in seconds). Note that both axes are log-scale. The mapping and routing algorithms are abbreviated in the legend here and in future figures such that the first part of the name represents the mapping algorithm and the second part represents the routing algorithm. For example, OPTIMAL-OPTIMAL is the full optimal encoding and STRUCT-GREEDY is STRUCT-MAP composed with GREEDY-ROUTE.

We see that, as expected, OPTIMAL-OPTIMAL is slower than any of the methods that sacrifice both optimal mapping and routing. The maximum depth of a circuit compiled within the timeout is 117. In fact, this is true of any method that applies optimal routing. We only show STRUCT-OPTIMAL on the chart, but the results are similar for other hybrid methods that combine efficient mapping with optimal routing. We observe better scaling in the algorithms that use GREEDY-ROUTE for routing, which all successfully compiled a circuit with a depth of at least 10,000. Also evident is the expected linear shift when comparing the runtime of RAND(20)-GREEDY to RAND(1)-GREEDY as the former is essentially performing the computation of the latter 20 times. RAND(1)-GREEDY and STRUCT-GREEDY exhibit similar scaling with circuit depth, suggesting that the additional computation of determining a structural placement is insignificant compared to the routing phase.

**Qubit count.** We are also interested in scaling in an orthogonal dimension: the number of qubits in the circuit. Among the application circuits, there is a limited range of qubit counts. The parameterized application circuits, such as the Shor’s algorithm circuits, can be instantiated with arbitrary qubit count, but not while keeping the depth fixed.

We fill this gap with randomly generated circuits. The results are shown in Fig. 11b. The random circuits are parameterized by qubit count and depth, with both variables ranging from 1 to 100. For the purpose of focusing on the qubit count in this plot, the circuit depth is fixed to 16. Similarly to the depth plot, the RAND(1)-GREEDY and STRUCT-GREEDY methods are the fastest and are essentially indistinguishable. Unlike in the depth plot, here we do observe some runtime gains from the

heuristic initial map of STRUCT-OPTIMAL over OPTIMAL-OPTIMAL. This makes intuitive sense as the SAT oracle invoked by OPTIMAL-OPTIMAL is essentially performing an exhaustive search over the possible maps, a space which scales exponentially with qubit count. Choosing a heuristic placement like in STRUCT-OPTIMAL avoids this source of exponential dependence on qubit count.

### (RQ2): How close to optimal are the solutions of relaxations?

*Summary: On application circuits, the distance from optimal is generally bounded by a 20% overhead. However, results on the known-optimal circuits suggest randomized methods perform poorly on dense inputs, producing solutions with several times the optimal number of time steps.*

Even given a fixed qubit map, optimal routing produces optimal or very nearly optimal results in all cases, so we focus on greedy routing. We separately consider the quality of solutions on the application circuits and the known-optimal circuits from Section 7.

**Application circuits.** For large application circuits, the OPTIMAL method cannot be applied, so we do not necessarily know the value of the optimal solution. However, as we have seen, we can always lower bound the number of time steps in optimal solution by the depth of the circuit. The depth bound motivates the *cost ratio* solution quality metric, defined as the quantity

$$\frac{\text{\# of time steps in solution}}{\text{depth of circuit}}$$

In Fig. 12, we plot the cost ratios on application circuits using *s-curves*, where each point corresponds to a circuit, and the points are arranged in increasing order of cost ratio. We plot the median solution from 5 trials for the randomized methods here and in all s-curves. We observe little variance between trials, with a maximum standard deviation across all circuits of 0.05 for RAND(20)-GREEDY and 0.14 for RAND(1)-GREEDY. The fractions to the right of the chart area count the number of benchmarks for which the depth lower-bound is achieved. We compare across the 138 circuits for which all relaxations were solved. The results are fairly uniform across the relaxations, with the most notable difference being the large proportion of circuits for which the RAND(20)-GREEDY method achieves the depth lower-bound (40%). Notice that this is the only method that explicitly computes a full gate route for multiple qubit maps. The favorable results suggest that for these circuits, selecting from multiple qubit maps is a stronger strategy than carefully computing a single candidate.

On the individual circuit level, we notice that the circuit implementing Grover’s algorithm is among the top three cost ratios for all three methods. The fact that this circuit induces the highest cost ratio for each method indicates that Grover’s algorithm circuits are good candidates for realistic circuits to use in stress-testing surface code mapping and routing procedures in future work.

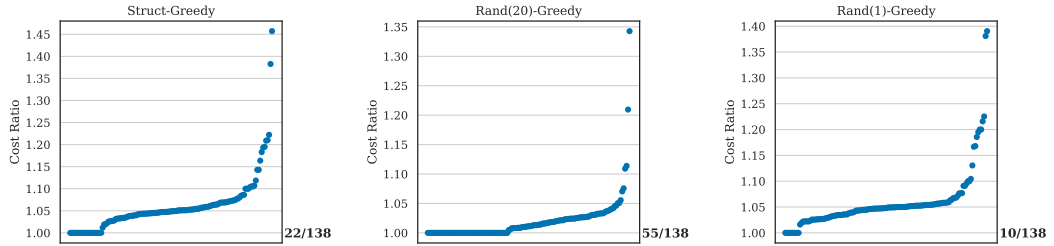


Fig. 12. Solution quality of greedy routing methods on application circuits

**Known-optimal circuits.** The results on the known-optimal circuits do differ significantly across the relaxations. Fig. 13 presents the cost ratios of the relaxation solutions for known-optimal

circuits with depth and qubit count ranging from 2 to 200. For each depth and qubit count pair, a circuit is generated with density 1/4, 1/2, 3/4, and 1. Here we notice a significant separation between the STRUCT-MAP, which is informed by the structure of the circuit, and the other methods, which are not. We see little effect from varying the density of the circuit and strong performance overall. The maximum cost ratio across all circuits for STRUCT-GREEDY is 1.5. On the other hand, for RAND(20)-GREEDY, we see a clear dependence on density and a significantly higher maximum ratio for full density circuits of 5.36. The discrepancy between structural and randomized methods in terms of their sensitivity to circuit density suggests structural methods may be better suited for compiling highly parallel circuits involving many independent gates between disjoint sets of qubits.

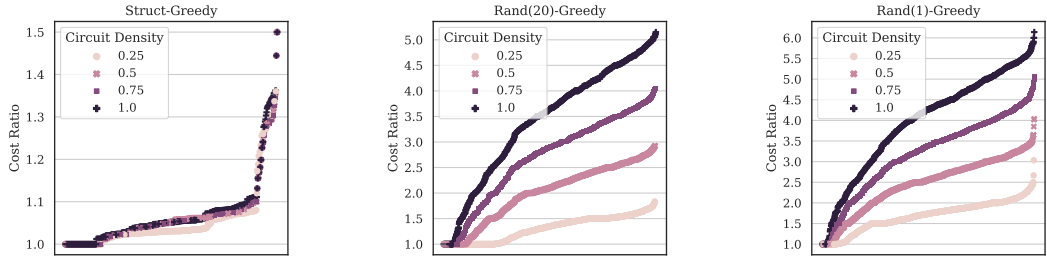


Fig. 13. Solution quality of greedy routing methods on known-optimal circuits

### (R3): What is the effect of varying magic state placement?

*Summary: We see little impact from restricting the magic states to one side or the center of the architecture as compared to our default assumption of magic states on along all sides.*

To address this question we consider two alternative target architectures: the *Right-Column Architecture* and the *Center-Column Architecture*. The Right-Column Architecture simply omits the magic state qubits on three of the sides, leaving only the rightmost column. The Center-Column Architecture includes a column of magic state qubits down the center of the grid, with vertices available for circuit qubits to the left and right.

The results for the compiling the application circuits to the Center-Column architecture are shown in Fig. 14 (they are similar for the Right-Column case). Overall, we notice that many of the same observations from our analysis of (RQ2). The consistency across architecture indicates that the fairly optimistic assumption of magic states available in all directions is a safe one as it does not have a major impact on the cost ratio across these circuits. Moreover, it suggests that our relaxations are generic and flexible.

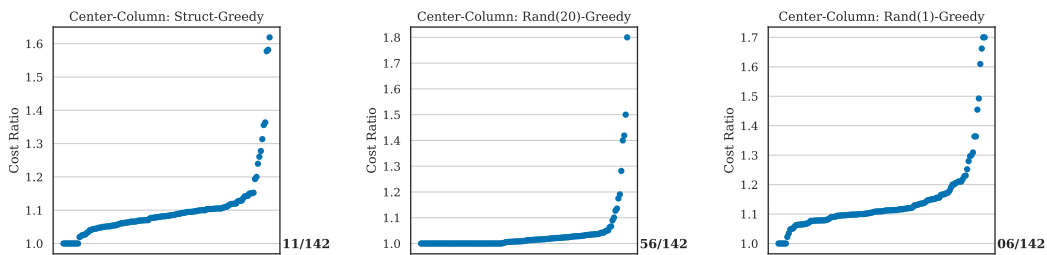


Fig. 14. Solution quality on the Center-Column Architecture

## 9 RELATED WORK

**Surface Code Compilation.** Some recent work in compilation for surface-encoded quantum devices has addressed similar problems to the surface code mapping and routing problem. Javadi-Abhari et al. [25] identifies CNOT contention as an important architectural design factor and develops heuristics for mapping qubits and scheduling CNOT gates implemented as defect braids, an alternative to lattice surgery. The central abstraction of finding vertex disjoint paths applies to both defect braiding and lattice surgery; we focus on lattice surgery based on evidence that it is a more resource-efficient approach [17]. Autobraid [23] builds on this work with an improved algorithm for qubit mapping that maximizes the number of groups of CNOT gates that can be simultaneously routed within the bounding box of the qubits they act on. However, neither consider CNOT gates induced by T gates or the constraints of lattice surgery CNOT gates. Beverland et al. [8] considers a similar greedy routing algorithm to our own, but assume a given fixed map that places qubits in a “checkerboard” structure. None of the above work provides an optimal solver for the compilation problem they address. Lao et al. [30] does solve a mapping and routing problem optimally with integer linear programming, but this formulation does not permit long-range CNOT gates. In terms of hardness results, optimizing the resource usage of lattice surgery has been proven NP-complete [21] in the context of a different execution paradigm [20] where circuits are first translated to a special form amenable to lattice surgery.

**NISQ Qubit Mapping and Routing.** A wide array of recent work has focused on the qubit mapping and CNOT routing problem for noisy intermediate-scale quantum computers without error-correction. Particularly relevant approaches includes those based on SAT/SMT like our OPTIMAL solver [31, 34, 43, 47] and those that construct qubit maps based on interaction graphs [40] or interaction chain sets [15] like STRUCT-MAP. In this setting, prior work has procedurally generated circuits with a known optimal solution to evaluate the quality of heuristic solutions [44], analogous to the circuits in Section 7.

**Other Allocation and Disjoint Paths Problems.** Surface code mapping and routing is a process that assigns program variables to limited physical resources such that the runtime efficiency is maximized, much like the classical problem of register allocation [11, 14, 35]. Disjoint paths problems like the constraints on a valid gate route have also been studied in other contexts including VLSI routing [3, 29] and all-optical networks [2, 6, 37]. Inspired by these applications, the study of approximation algorithms for disjoint path problems is an active area with both hardness results [4, 16] and approximation algorithms on planar graphs [13] and grid graphs [12]. However, a distinguishing feature of this particular problem that separates it from other disjoint path problems is the dependency between paths, which forces routing certain pairs in a particular order.

## 10 CONCLUSIONS

In this paper, we have developed a theoretical framework for surface code mapping and routing, a critical problem in compilation for emerging practical quantum computers. We explored the space of solutions and identified some practical algorithms which our results show provide high quality solutions in reasonable time. In future work, we plan to extend our model and algorithms to capture a broader class of quantum architectures. For example, we could relax the assumption that availability of magic states is not a limiting factor and explicitly model the bandwidth of magic state production. Another direction is to support recent designs for heterogeneous multi-chip fault-tolerant quantum architectures [41, 42]. The mapping and routing problem in this case is nuanced because not all CNOT gates are equivalent. If the two qubits are located on different chips, a CNOT gate is possible, but more costly.

## REFERENCES

- [1] Rajeev Acharya, I. Aleiner, Richard Allen, Trond I. Andersen, Markus Ansmann, Frank Arute, Kunal Arya, Abraham T. Asfaw, Juan Atalaya, Ryan Babbush, Dave Bacon, Joseph C. Bardin, João Basso, Andreas Bengtsson, Sergio Boixo, Gina Bortoli, Alexandre Bourassa, Jenna Bovaird, Leon Brill, Mick Broughton, Bob B Buckley, David A. Buell, Tim Burger, Brian Burkett, Nicholas Bushnell, Yu Chen, Zijun Chen, Benjamin Chiaro, J. Zachery Cogan, Roberto Collins, P. N. Conner, William Courtney, Alexander L. Crook, Benjamin M. Curtin, Dripto M. Debroy, Alexander Del Toro Barba, Sean Demura, Andrew Dunsworth, Daniel Eppens, Catherine Erickson, Lara Faoro, Edward Farhi, Reza Fatemi, Leslie Flores Burgos, Ebrahim Forati, Austin G. Fowler, Brooks Foxen, William Giang, Craig Gidney, Dar Gilboa, Marissa Giustina, Alejandro Grajales Dau, Jonathan A. Gross, S. Habegger, Michael C. Hamilton, Matthew P. Harrigan, Sean D. Harrington, Oscar Higgott, Jeremy P. Hilton, Michael J. Hoffmann, Sabrina Hong, Trent Huang, Ashley Huff, William J. Huggins, L. B. Ioffe, Sergei V. Isakov, Justin Iveland, Evan Jeffrey, Zhang Jiang, Cody Jones, Pavol Juhás, Dvir Kafri, Kostyantyn Kechedzhi, Julian Kelly, Tanuj Khattar, Mostafa Khezri, M’aria Kieferov’á, Seon Kim, Alexei Kitaev, Paul V. Klimov, Andrey R. Klots, Alexander N. Korotkov, Fedor Kostritsa, John Mark Kreikebaum, David Landhuis, Pavel Laptev, Kim Ming Lau, Lily Laws, Joonho Lee, Kenny Lee, Brian J. Lester, Alexander T Lill, Wayne Liu, Aditya Locharla, Erik Lucero, Fionn D. Malone, Jeffrey Marshall, Orion Martin, Jarrod R. McClean, Trevor McCourt, Matthew J. McEwen, Anthony Megrant, Bernardo Meurer Costa, Xiao Mi, Kevin C. Miao, Masoud Mohseni, Shirin Montazeri, Alexis Morvan, Emily Mount, Wojciech Mruczkiewicz, Ofer Naaman, Matthew Neeley, Charles J.Neill, Ani Nersisyan, Hartmut Neven, Michael Newman, J. H. Ng, Anthony Nguyen, Murray L. Nguyen, Murphy Yuezhen Niu, Thomas E. O’Brien, Alexander Opremcak, J. Platt, Andre Petukhov, Rebecca Potter, Leonid P. Pryadko, Chris Quintana, Pedram Roushan, Nicholas C. Rubin, Negar Saei, Daniel Thomas Sank, Kannan A. Sankaragomathi, Kevin J. Satzinger, Henry F. Schurkus, C. Schuster, Michael Shearn, Aaron Shorter, Vladimir Shvarts, Jindra Skrzyn, Vadim N. Smelyanskiy, William C. Smith, George Sterling, Doug Strain, Yuan Su, Marco Szalay, Alfredo Torres, Guifre Vidal, Benjamin Villalonga, C. V. Heidweiller, Theodore White, Chen Xing, Z. Jamie Yao, Ping Yeh, Juhwan Yoo, Grayson Young, Adam Zalcman, Yaxing Zhang, and Ningfeng Zhu. 2022. Suppressing quantum errors by scaling a surface code logical qubit. *Nature* 614 (2022), 676 – 681. <https://api.semanticscholar.org/CorpusID:250526184>
- [2] Alok Aggarwal, Amotz Bar-Noy, Don Coppersmith, Rajiv Ramaswami, Baruch Schieber, and Madhu Sudan. 1994. Efficient Routing and Scheduling Algorithms for Optical Networks. In *Proceedings of the Fifth Annual ACM-SIAM Symposium on Discrete Algorithms* (Arlington, Virginia, USA) (SODA ’94). Society for Industrial and Applied Mathematics, USA, 412–423.
- [3] Alok Aggarwal, Jon Kleinberg, and David P. Williamson. 2000. Node-Disjoint Paths on the Mesh and a New Trade-Off in VLSI Layout. *SIAM J. Comput.* 29, 4 (2000), 1321–1333. <https://doi.org/10.1137/S0097539796312733> arXiv:<https://doi.org/10.1137/S0097539796312733>
- [4] M. Andrews, J. Chuzhoy, Sanjeev Khanna, and L. Zhang. 2005. Hardness of the undirected edge-disjoint paths problem with congestion. In *46th Annual IEEE Symposium on Foundations of Computer Science (FOCS’05)*. 226–241. <https://doi.org/10.1109/SFCS.2005.41>
- [5] Carlos Ansótegui and Felip Manyà. 2004. Mapping problems with finite-domain variables into problems with boolean variables. 1–15.
- [6] Yonatan Aumann and Yuval Rabani. 1995. Improved Bounds for All Optical Routing. In *Proceedings of the Sixth Annual ACM-SIAM Symposium on Discrete Algorithms* (San Francisco, California, USA) (SODA ’95). Society for Industrial and Applied Mathematics, USA, 567–576.
- [7] Olivier Bailleux and Yacine Boufkad. 2003. Efficient CNF Encoding of Boolean Cardinality Constraints. In *International Conference on Principles and Practice of Constraint Programming*. <https://api.semanticscholar.org/CorpusID:8967694>
- [8] Michael Beverland, Vadym Kliuchnikov, and Eddie Schoute. 2022. Surface Code Compilation via Edge-Disjoint Paths. *PRX Quantum* 3 (May 2022), 020342. Issue 2. <https://doi.org/10.1103/PRXQuantum.3.020342>
- [9] Armin Biere, Katalin Fazekas, Mathias Fleury, and Maximilian Heisinger. 2020. CaDiCaL, Kissat, Paracooba, Plingeling and Treengeling Entering the SAT Competition 2020. In *Proc. of SAT Competition 2020 – Solver and Benchmark Descriptions (Department of Computer Science Report Series B, Vol. B-2020-1)*, Tomas Balyo, Nils Froleyks, Marijn Heule, Markus Iser, Matti Järvisalo, and Martin Suda (Eds.). University of Helsinki, 51–53.
- [10] Sergey Bravyi and Alexei Kitaev. 2005. Universal quantum computation with ideal Clifford gates and noisy ancillas. *Physical Review A* 71, 2 (Feb 2005). <https://doi.org/10.1103/physreva.71.022316>
- [11] G. J. Chaitin. 1982. Register Allocation & Spilling via Graph Coloring. *SIGPLAN Not.* 17, 6 (jun 1982), 98–101. <https://doi.org/10.1145/872726.806984>
- [12] Julia Chuzhoy and David H. K. Kim. 2015. On Approximating Node-Disjoint Paths in Grids. In *Approximation, Randomization, and Combinatorial Optimization. Algorithms and Techniques (APPROX/RANDOM 2015) (Leibniz International Proceedings in Informatics (LIPIcs), Vol. 40)*, Naveen Garg, Klaus Jansen, Anup Rao, and José D. P. Rolim (Eds.). Schloss Dagstuhl–Leibniz-Zentrum fuer Informatik, Dagstuhl, Germany, 187–211. <https://doi.org/10.4230/LIPIcs.APPROX-RANDOM.2015.187>

- [13] Julia Chuzhoy, David H. K. Kim, and Shi Li. 2016. Improved Approximation for Node-Disjoint Paths in Planar Graphs. In *Proceedings of the Forty-Eighth Annual ACM Symposium on Theory of Computing* (Cambridge, MA, USA) (STOC '16). Association for Computing Machinery, New York, NY, USA, 556–569. <https://doi.org/10.1145/2897518.2897538>
- [14] Keith D. Cooper and Linda Torczon. 2023. Chapter 13 - Register Allocation. In *Engineering a Compiler (Third Edition)* (third edition ed.), Keith D. Cooper and Linda Torczon (Eds.). Morgan Kaufmann, Philadelphia, 663–712. <https://doi.org/10.1016/B978-0-12-815412-0.00019-X>
- [15] Alexander Cowtan, Silas Dilkes, Ross Duncan, Alexandre Krajenbrink, Will Simmons, and Seyon Sivarajah. 2019. On the qubit routing problem. *arXiv preprint arXiv:1902.08091* (2019).
- [16] Thomas Erlebach. 2006. Approximation Algorithms for Edge-Disjoint Paths and Unsplittable Flow. In *Efficient Approximation and Online Algorithms - Recent Progress on Classical Combinatorial Optimization Problems and New Applications*, Evripidis Bampis, Klaus Jansen, and Claire Kenyon (Eds.). Lecture Notes in Computer Science, Vol. 3484. Springer, 97–134. [https://doi.org/10.1007/11671541\\_4](https://doi.org/10.1007/11671541_4)
- [17] Austin G. Fowler and Craig Gidney. 2018. Low overhead quantum computation using lattice surgery. *arXiv: Quantum Physics* (2018).
- [18] Austin G. Fowler, Matteo Mariantoni, John M. Martinis, and Andrew N. Cleland. 2012. Surface codes: Towards practical large-scale quantum computation. *Physical Review A* 86, 3 (sep 2012). <https://doi.org/10.1103/physreva.86.032324>
- [19] Ian P. Gent and Peter Nightingale. 2004. A new encoding of All Different into SAT. In *International Workshop on Modelling and Reformulating Constraint Satisfaction Problems*.
- [20] Daniel Herr, Franco Nori, and Simon J Devitt. 2017. Lattice surgery translation for quantum computation. *New Journal of Physics* 19, 1 (jan 2017), 013034. <https://doi.org/10.1088/1367-2630/aa5709>
- [21] Daniel Herr, Franco Nori, and Simon J. Devitt. 2017. Optimization of lattice surgery is NP-hard. *npj Quantum Information* 3, 1 (oct 2017). <https://doi.org/10.1038/s41534-017-0035-1>
- [22] Clare Horsman, Austin G Fowler, Simon Devitt, and Rodney Van Meter. 2012. Surface code quantum computing by lattice surgery. *New Journal of Physics* 14, 12 (dec 2012), 123011. <https://doi.org/10.1088/1367-2630/14/12/123011>
- [23] Fei Hua, Yanhao Chen, Yuwei Jin, Chi Zhang, Ari Hayes, Youtao Zhang, and Eddy Z. Zhang. 2021. AutoBraid: A Framework for Enabling Efficient Surface Code Communication in Quantum Computing. In *MICRO-54: 54th Annual IEEE/ACM International Symposium on Microarchitecture* (Virtual Event, Greece) (MICRO '21). Association for Computing Machinery, New York, NY, USA, 925–936. <https://doi.org/10.1145/3466752.3480072>
- [24] Alexey Ignatiev, Antonio Morgado, and Joao Marques-Silva. 2018. PySAT: A Python Toolkit for Prototyping with SAT Oracles. In *SAT*. 428–437. [https://doi.org/10.1007/978-3-319-94144-8\\_26](https://doi.org/10.1007/978-3-319-94144-8_26)
- [25] Ali Javadi-Abhari, Pranav Gokhale, Adam Holmes, Diana Franklin, Kenneth R. Brown, Margaret Martonosi, and Frederic T. Chong. 2017. Optimized Surface Code Communication in Superconducting Quantum Computers. In *Proceedings of the 50th Annual IEEE/ACM International Symposium on Microarchitecture* (Cambridge, Massachusetts) (MICRO-50 '17). Association for Computing Machinery, New York, NY, USA, 692–705. <https://doi.org/10.1145/3123939.3123949>
- [26] Jon M. Kleinberg. 1996. Approximation algorithms for disjoint paths problems. <https://api.semanticscholar.org/CorpusID:45695383>
- [27] Emanuel Knill, Raymond Laflamme, and Wojciech H. Zurek. 1998. Resilient quantum computation: error models and thresholds. *Proceedings of the Royal Society of London. Series A: Mathematical, Physical and Engineering Sciences* 454, 1969 (jan 1998), 365–384. <https://doi.org/10.1098/rspa.1998.0166>
- [28] Stavros G. Kolliopoulos and Clifford Stein. 1997. Approximating Disjoint-Path Problems Using Greedy Algorithms and Packing Integer Programs. In *Conference on Integer Programming and Combinatorial Optimization*. <https://api.semanticscholar.org/CorpusID:8670709>
- [29] M.R Kramer and J van Leeuwen. 1984. The complexity of wire-routing and finding minimum area layouts for arbitrary vlsi circuits. *Advances in computing research* 2 (1984), 020342.
- [30] L Lao, B van Wee, I Ashraf, J van Someren, N Khammassi, K Bertels, and C G Almudever. 2018. Mapping of lattice surgery-based quantum circuits on surface code architectures. *Quantum Science and Technology* 4, 1 (sep 2018), 015005. <https://doi.org/10.1088/2058-9565/aadd1a>
- [31] Wan-Hsuan Lin, Jason Kimko, Bochen Tan, Nikolaj S. Bjørner, and Jason Cong. 2023. Scalable Optimal Layout Synthesis for NISQ Quantum Processors. *2023 60th ACM/IEEE Design Automation Conference (DAC)* (2023), 1–6. <https://api.semanticscholar.org/CorpusID:260688265>
- [32] Daniel Litinski. 2018. A Game of Surface Codes: Large-Scale Quantum Computing with Lattice Surgery. *Quantum* (2018).
- [33] Daniel Litinski and Felix von Oppen. 2018. Lattice Surgery with a Twist: Simplifying Clifford Gates of Surface Codes. *Quantum* 2 (May 2018), 62. <https://doi.org/10.22331/q-2018-05-04-62>
- [34] Abtin Molavi, Amanda Xu, Martin Diges, Lauren Pick, Swamit S. Tannu, and Aws Albarghouthi. 2022. Qubit Mapping and Routing via MaxSAT. *2022 55th IEEE/ACM International Symposium on Microarchitecture (MICRO)* (2022), 1078–1091.

<https://api.semanticscholar.org/CorpusID:251903259>

- [35] Massimiliano Poletto and Vivek Sarkar. 1999. Linear Scan Register Allocation. *ACM Trans. Program. Lang. Syst.* 21, 5 (sep 1999), 895–913. <https://doi.org/10.1145/330249.330250>
- [36] Steven Prestwich. 2009. CNF encodings. *Frontiers in Artificial Intelligence and Applications* 185 (01 2009). <https://doi.org/10.3233/978-1-58603-929-5-75>
- [37] Prabhakar Raghavan and Eli Upfal. 1994. Efficient Routing in All-Optical Networks. In *Proceedings of the Twenty-Sixth Annual ACM Symposium on Theory of Computing* (Montreal, Quebec, Canada) (STOC '94). Association for Computing Machinery, New York, NY, USA, 134–143. <https://doi.org/10.1145/195058.195119>
- [38] C. Ryan-Anderson, J. G. Bohnet, K. Lee, D. Gresh, A. Hankin, J. P. Gaebler, D. Francois, A. Chernoguzov, D. Lucchetti, N. C. Brown, T. M. Gatterman, S. K. Halit, K. Gilmore, J. A. Gerber, B. Neyenhuis, D. Hayes, and R. P. Stutz. 2021. Realization of Real-Time Fault-Tolerant Quantum Error Correction. *Phys. Rev. X* 11 (Dec 2021), 041058. Issue 4. <https://doi.org/10.1103/PhysRevX.11.041058>
- [39] Carsten Sinz. 2005. Towards an Optimal CNF Encoding of Boolean Cardinality Constraints. In *International Conference on Principles and Practice of Constraint Programming*. <https://api.semanticscholar.org/CorpusID:8151957>
- [40] Marcos Yukio Siraichi, Vinícius Fernandes dos Santos, Caroline Collange, and Fernando Magno Quintão Pereira. 2019. Qubit allocation as a combination of subgraph isomorphism and token swapping. *Proceedings of the ACM on Programming Languages* 3, OOPSLA (2019), 1–29.
- [41] K. N. Smith, G. Ravi, J. M. Baker, and F. T. Chong. 2022. Scaling Superconducting Quantum Computers with Chiplet Architectures. In *2022 55th IEEE/ACM International Symposium on Microarchitecture (MICRO)*. IEEE Computer Society, Los Alamitos, CA, USA, 1092–1109. <https://doi.org/10.1109/MICRO56248.2022.00078>
- [42] Samuel Stein, Sara Sussman, Teague Tomesh, Charles Guinn, Esin Tureci, Sophia Fuhui Lin, Wei Tang, James Ang, Srivatsan Chakram, Ang Li, Margaret Martonosi, Fred T. Chong, Andrew A. Houck, Isaac L. Chuang, and Michael Austin DeMarco. 2023. HetArch: Microarchitectures for Heterogeneous Superconducting Quantum Computers. In *2023 56th IEEE/ACM International Symposium on Microarchitecture (MICRO)*. arXiv:2305.03243 [quant-ph]
- [43] Bochen Tan and Jason Cong. 2020. Optimal Layout Synthesis for Quantum Computing. In *Proceedings of the 39th International Conference on Computer-Aided Design* (Virtual Event, USA) (ICCAD '20). Association for Computing Machinery, New York, NY, USA, Article 137, 9 pages. <https://doi.org/10.1145/3400302.3415620>
- [44] Bochen Tan and Jason Cong. 2020. Optimality study of existing quantum computing layout synthesis tools. *IEEE Trans. Comput.* 70, 9 (2020), 1363–1373.
- [45] J.D. Ullman. 1975. NP-complete scheduling problems. *J. Comput. System Sci.* 10, 3 (1975), 384–393. [https://doi.org/10.1016/S0022-0008\(75\)80008-0](https://doi.org/10.1016/S0022-0008(75)80008-0)
- [46] George Watkins, Hoang Minh Nguyen, Varun Seshadri, Keelan Watkins, Steven Pearce, Hoi-Kwan Lau, and Alexandru Paler. 2023. A High Performance Compiler for Very Large Scale Surface Code Computations. arXiv:2302.02459 [quant-ph]
- [47] Robert Wille, Lukas Burgholzer, and Alwin Zulehner. 2019. Mapping Quantum Circuits to IBM QX Architectures Using the Minimal Number of SWAP and H Operations. *2019 56th ACM/IEEE Design Automation Conference (DAC)* (2019), 1–6. <https://api.semanticscholar.org/CorpusID:163164939>
- [48] Robert Wille, Daniel Große, Lisa Teuber, Gerhard W. Dueck, and Rolf Drechsler. 2008. RevLib: An Online Resource for Reversible Functions and Reversible Circuits. In *38th International Symposium on Multiple Valued Logic (ismvl 2008)*, 220–225. <https://doi.org/10.1109/ISMVL.2008.43>
- [49] Youwei Zhao, Yangsen Ye, He-Liang Huang, Yiming Zhang, Dachao Wu, Huijie Guan, Qingling Zhu, Zuolin Wei, Tan He, Sirui Cao, Fusheng Chen, Tung-Hsun Chung, Hui Deng, Daojin Fan, Ming Gong, Cheng Guo, Shaojun Guo, Lianchen Han, Na Li, Shaowei Li, Yuan Li, Futian Liang, Jin Lin, Haoran Qian, Hao Rong, Hong Su, Lihua Sun, Shiyu Wang, Yulin Wu, Yu Xu, Chong Ying, Jiale Yu, Chen Zha, Kaili Zhang, Yong-Heng Huo, Chao-Yang Lu, Cheng-Zhi Peng, Xiaobo Zhu, and Jian-Wei Pan. 2022. Realization of an Error-Correcting Surface Code with Superconducting Qubits. *Phys. Rev. Lett.* 129 (Jul 2022), 030501. Issue 3. <https://doi.org/10.1103/PhysRevLett.129.030501>

## A SURFACE CODE ROUTING IS HARD

In this section, we prove Theorem 4.2.

The key idea of this reduction is a pair of constructions called vertex gadgets shown in Fig. 15. The *empty vertex gadget* on the left is used to represent vertices that are not included in the set of vertex pairs in the given NDP instance. The grey filled-in vertices are magic state qubits, which cannot be used to route gates. The *full vertex gadget* on the right is used to represent vertices that are not included in the set of vertex pairs in the given NDP instance. The center vertex (in blue) and the two green vertices diagonal to it are locations where we will map qubits from the circuit we will construct in the reduction. In particular, we will apply CNOT gates between qubits mapped to the center vertices of different full vertex gadgets and between qubits mapped to the diagonal vertices of the same full vertex gadget. For this reason, we refer to the diagonal vertices as the *internal* locations. As before, the other grey filled-in vertices are magic state qubits.



Fig. 15. Vertex gadgets

With these gadgets in hand we can describe the reduction. Let  $\text{NDP}(G, \mathcal{R})$  be an instance of NDP where  $\mathcal{R} = \{(s_1, t_1), \dots, (s_k, t_k)\}$ . We may assume that each vertex appears in at most one pair in  $\mathcal{R}$  as otherwise there is trivially no solution. We will now construct the corresponding SCR instance  $\text{SCR}(A, C, M, t_s)$ . First, set  $t_s = 1$ . If  $G$  is an  $n \times m$  grid, then  $A$  is chosen to be a  $n \times m$  grid of vertex gadgets. In this grid of gadgets, the gadget in grid position  $(r, c)$  is the full vertex gadget if vertex  $(r, c) \in G$  is in some pair in  $\mathcal{R}$ ; otherwise, it is the empty vertex gadget. This process is illustrated in Fig. 16 for the  $2 \times 2$  grid and  $\mathcal{R}$  consisting of a single pair  $((1, 1), (2, 2))$ . The solid regions in the figure consist entirely of magic state qubits. The circuit  $C$  includes one “external” CNOT gate  $\text{CNOT } \text{src}_i \text{ tar}_i$  for each pair  $(s_i, t_i) \in \mathcal{R}$ . The map  $M$  associates these gates with the proper vertices by mapping  $\text{src}_i$  to the center vertex of the gadget for  $s_i$ , and mapping  $\text{tar}_i$  to the center vertex of the gadget for  $t_i$ . The circuit  $C$  also includes one “internal” CNOT gate  $\text{CNOT } \text{tr}_v \text{ bl}_v$  for each vertex  $v$  that appears in a pair in  $\mathcal{R}$ , and  $M$  maps  $\text{tr}_v$  to the top-right internal location in the gadget for  $v$  and maps  $\text{bl}_v$  to the bottom-left internal location in the gadget for  $v$ . For the same simple example, this results in three CNOT gates over three disjoint pairs of qubits.

Next, we show that the answer to  $\text{SCR}(A, C, M, t_s)$  is “yes” if and only if the answer to  $\text{NDP}(G, \mathcal{R})$  is “yes.” The intuition behind the correspondence is shown in Fig. 17, using an solution to our running example.

First suppose there is some set  $\mathcal{P}$  of vertex-disjoint paths for routing the pairs in  $\mathcal{R}$ . For the external gates, we can construct a set of vertex-disjoint paths between the gadgets containing their qubits based on  $\mathcal{P}$ . In particular, the route for a gate  $\text{CNOT } \text{src}_i \text{ tar}_i$ , visits a vertex gadget if and only if the corresponding vertex is included in the routing for  $(s_i, t_i)$  in  $\mathcal{P}$ , and traverses them in the same order. Then, the final edge of the path can be made to have the right orientation by

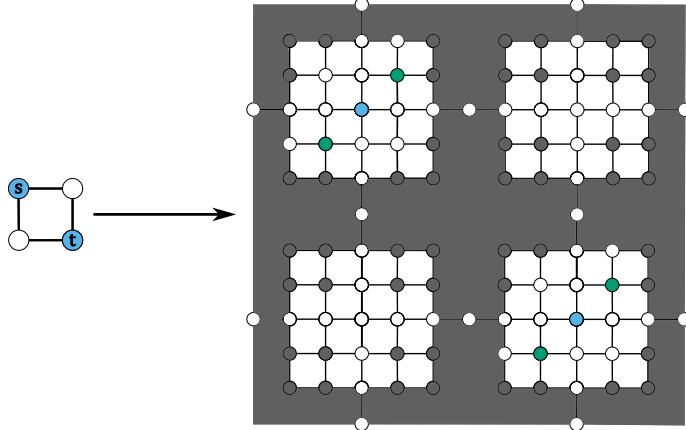


Fig. 16. Illustration of the reduction

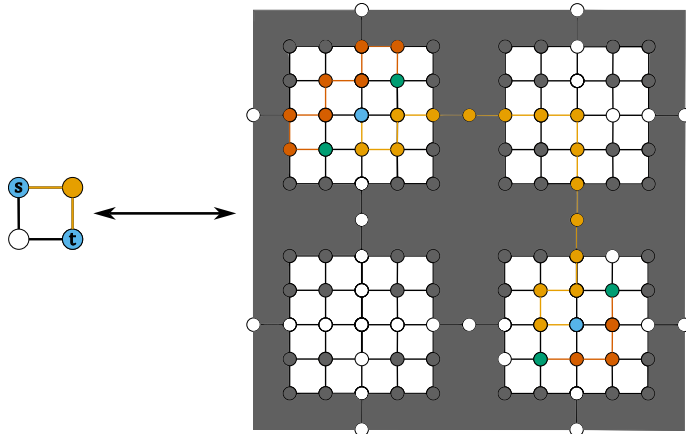


Fig. 17. Correspondence between solutions to the two problems

including vertices within the full vertex gadgets at the end points. The internal CNOT gates can be simultaneously be routed using other vertices within the gadget.

Now conversely suppose there is a valid gate route for  $A$ ,  $C$  and  $M$ . We claim the routing for two different external CNOT gates cannot use vertices in the same vertex gadget. Suppose for the sake of contradiction that the routes for two different gates include vertices from the same vertex gadget. This cannot be an empty vertex gadget because any path that visits an empty vertex gadget must include the center vertex, but, by definition, valid gate routes are vertex disjoint. Therefore, the two paths must both visit the same full vertex gadget corresponding to some vertex  $v$ . In the case, at least one of them must not terminate in this gadget, meaning it enters from and adjacent gadget and exits to another adjacent gadget. However, such a path in conjunction with the route for the external CNOT gate which does terminate at this gadget make it impossible to route the internal gate CNOT  $\text{tr}_v \text{ bl}_v$ . Thus, we have reached a contradiction. Now that we have established that at most one gate route can visit each vertex gadget, we can construct vertex-disjoint paths for the pairs in  $\mathcal{R}$  by inverting the process described in the previous direction, where the sequence of

vertices used in the path for the pair  $(s_i, t_i)$  is exactly the vertices corresponding to the sequence of gadgets used in the route for the gate CNOT  $\text{src}_i$   $\text{tar}_i$ .

## B SURFACE CODE MAPPING AND ROUTING IS HARD

In this section, we provide a self-contained full proof of Theorem 4.1, following the overview from Section 4.

### B.1 The Dependency Circuit

We begin with the *dependency circuit*: a structure that encodes the partial order on jobs as a circuit. This is nontrivial because the dependency structure allowed in a PSP instance is more general than that of quantum circuits.

To simulate an arbitrary dependency structure under this limitation, we use a construction called a *job gadget*. The job gadget is designed such that the T gate qubit inherits the incoming and outgoing dependencies of all of the other qubits. In general, the job gadget for a PSP instance  $J$  includes  $d + 1$  qubits, where  $d$  is the maximum degree of any job in the Hasse diagram of  $J$ . One of these qubits is used to execute a T gate that represents the job itself, and the rest are used to introduce dependencies with other job gadgets. Let  $q_{j,i}$  denote the  $i$ th qubit in the job gadget for  $j$ . The job gadget consists of the gates CNOT  $q_{j,0} q_{j,i}$  for each  $1 \leq i \leq d$ , then the gate T  $q_{j,0}$ , and finally a repetition of the gates CNOT  $q_{j,0} q_{j,i}$  for each  $1 \leq i \leq d$ .

For each job  $j$  we assign an indexing to the incoming and outgoing edges. Then, for each edge  $e = (j, j')$  we include the gate CNOT  $q_{j,i} q_{j',i'}$  between the job gadgets for  $j$  and  $j'$ , where  $i$  is the index of  $e$  as an outgoing edge of  $j$  and  $i'$  is its index as an incoming edge of  $j'$ . Notice that this ensures the gate T  $q_{j,0}$  must be executed before the gate T  $q_{j',0}$  as desired. We let  $\text{Dep}(J)$  denote the dependency circuit for a job set  $J$  and state this formally as Lemma B.1, where  $\prec^*$  is the transitive closure of the relation  $g \prec_C g'$  on gates in a circuit which says  $g'$  depends on  $g$ .

**LEMMA B.1.** *Let  $(J, \prec_J)$  be a partially ordered set. For each pair of jobs  $j, j' \in J$ , the T gate T  $q_{j,0}$  in  $\text{Dep}(J)$  satisfies the property that T  $q_{j,0} \prec^* T q_{j',0}$  if and only  $j \prec_J j'$ .*

**PROOF.** First suppose  $j \prec_J j'$ . We can induct on the length of the path from  $j$  to  $j'$  in the Hasse diagram for  $J$ . If the length of the path is 1, there are CNOT gates  $g_1 = \text{CNOT } q_{j,0} q_{j,i}$ ,  $g_2 = \text{CNOT } q_{j,i} q_{j',i'}$ , and  $g_3 = \text{CNOT } q_{j',0} q_{j',i'}$ , such that T  $q_{j,0} \prec_C g_1 \prec_C g_2 \prec_C g_3 \prec_C T q_{j',0}$ . Thus, T  $q_{j,0} \prec^* T q_{j',0}$ . If the length of the path is greater than 1, with final edge  $(j_k, j')$ , then by the above argument, T  $q_{j_k,0} \prec^* T q_{j',0}$ , and by induction, T  $q_{j,0} \prec^* T q_{j_k,0}$ . By transitivity, T  $q_{j,0} \prec^* T q_{j',0}$ .

Now assume T  $q_{j,0} \prec^* T q_{j',0}$ . Then there is a chain T  $q_{j,0} \prec_C g_1 \prec_C \dots \prec_C g_k \prec_C T q_{j',0}$ . We can similarly proceed by induction on the number of T gates among the gates  $g_1 \dots g_k$ . If there are none, then  $(j, j')$  is an edge in the Hasse diagram for  $J$ . Now suppose there are  $k$  such gates, with the last one between a qubit in the job gadget for job  $j_k$  and the job gadget for  $j'$ . Then, by the base case, there is an edge  $(j_k, j)$  in the Hasse diagram, by induction,  $j \prec_J j_k$  and by transitivity  $j \prec_J j'$ .  $\square$

### B.2 The Cycle Circuit

**Choosing the time limit.** If  $d$  is the maximum in-degree or out-degree of any job, we need  $2d + 1$  time steps to execute a job gadget. First, we execute  $d$  CNOT gates, then the T gate, then  $d$  more CNOT gates. Therefore, each time step in a PSP instance will need to be “stretched” into  $2d + 1$  time steps in a corresponding SCMR instance.

Additionally, between time steps  $t$  and  $t + 1$ , we must perform up to  $dk$  CNOT gates connecting the job gadgets executed in step  $t$  to those that depend upon them. These cross the architecture, so in the worst case we need to execute them sequentially, for  $dk$  time steps per transition. There are  $t_p - 1$  transitions between  $t_p$  time steps. Thus, we set the time limit  $t_s = (2d + 1)t_p + (dk)(t_p - 1)$ .

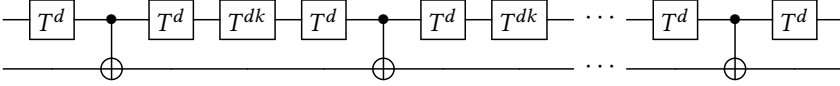


Fig. 18. Fragment of the cycle circuit. There is one layer of CNOT gates for each time step in the PSP instance and one copy of this two-qubit circuit per processor. The notation  $\tau^x$  means  $x$  copies of the  $\tau$  gate.

**The cycle circuit.** Extending the time limit as described above preserves PSP solutions, but it also could introduce spurious solutions to the SCMR instance that involve executing  $\tau$  gates “between” time steps and have no corresponding PSP schedule. The problem is that stretching the time steps has allowed squeezing multiple  $\tau$  gates into different steps in a range intended to represent a single PSP step.

The next key component of the proof is another circuit **on a distinct register of qubits** designed to disallow such solutions. We call this the *cycle circuit* because it consists of a repeating pattern of  $\tau$  gates to occupy the magic state qubits, so that there are only  $t$  steps in which  $\tau$  gates from the dependency circuit can be performed. For each of the  $k$  processors, we include  $t$  cycles. Each cycle consists of the following pattern:

- $d$   $\tau$  gates
- A CNOT gate
- $d$  more  $\tau$  gates.

Between cycles we include  $dk$   $\tau$  gates as well. We denote the cycle circuit with parameters  $d, k$ , and  $t_p$  as  $\text{Cycle}(d, k, t_p)$ . Lemma B.2 says that we can use the cycle circuit to restrict the dependency circuit to executing  $\tau$  gates during the  $t$  time steps where the cycle circuit executes CNOT gates.

**LEMMA B.2.** *Any scheduling for  $\text{Cycle}(J, k, t_p)$  in  $t_s = (2d + 1)t_p + (dk)(t_p - 1)$  time steps includes  $t$  time steps where no  $\tau$  gates are executed with  $dk$  time steps where  $k$   $\tau$  gates are executed interspersed between each.*

**PROOF.** Since each gate is part of a chain of  $t_s$  dependent operations, it must be executed at the time step corresponding to its position  $i$  in the chain. It cannot be executed in an earlier time step because either  $i = 1$  or there are  $i - 1$  steps necessary to execute the gates which precede it. It cannot be executed in a later time step because then the last gate in its chain will not be executed within the  $t_s$  step limit. There are  $t_s$  positions where all  $k$  chains of dependent operations in  $\text{Cycle}(J, k, t_s)$  include a CNOT gate, and thus  $t$  time steps where  $k$  CNOT gates are executed (and no  $\tau$  gates). Moreover, these positions are separated by  $dk$  positions where each chain includes a  $\tau$  gate, for  $k$  total simultaneous  $\tau$  gates.  $\square$

### B.3 Architecture

The processor unit for this example is shown in Fig. 19. The yellow vertex (third row, second column from the right) is the magic state qubit. The other colored vertices represent the mapping that will be used in one direction of the proof of the correctness of the reduction. Along the top row we map the 4 qubits of each job gadget together. There are as many such slots as jobs, to allow as many jobs to be mapped to this processor as desired. The two pink qubits (near the magic state qubit) are a pair from the cycle circuit. In total, a processor unit is a  $4 \times 6|J| + 1$  grid (the additional column is for connecting processor units) with one magic state qubit in the second row from the bottom and second column from the right.

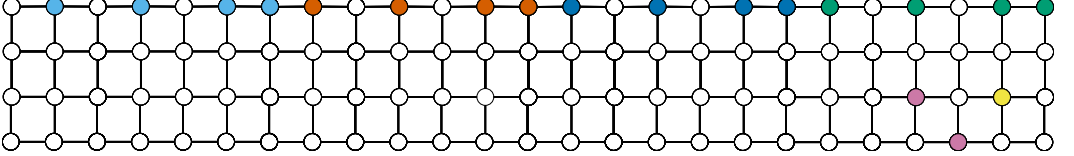


Fig. 19. Processor unit for our running example.

#### B.4 Putting it all together

We are now ready to describe the full reduction from  $\text{PSP}$  to  $\text{SCMR}$ . Let  $\text{PSP}(J, k, t_p)$  denote a  $\text{PSP}$  instance and let  $d$  be the maximum in-degree or out-degree of any job in  $J$ . We construct the corresponding  $\text{SCMR}$  instance,  $\text{SCMR}(A, C, t_s)$  as follows. Set  $A$  to consist of  $k$  processor units. Set  $C$  to be composed of two parallel, independent subcircuits:  $\text{Dep}(J)$  acting on a qubit set  $Q$  and  $\text{Cycle}(J, k, t)$  acting on a distinct set  $Q'$ . Set  $t_s = (2d + 1)t_p + (t_p - 1)(dk)$ .

Suppose the answer to  $\text{PSP}(J, k, t_p)$  is “yes.” Let  $s$  be a corresponding schedule. We can construct a solution  $s'$  for  $\text{SCMR}(A, C, t_s)$  from  $s$ . For the mapping, we map the qubits from a job gadget to the processor unit corresponding to the processor on which the job is executed in  $s$ . One pair of qubits from the cycle circuit is mapped to each processor unit as well. A valid gate route for the cycle circuit under this mapping can be constructed by executing each gate at the time step equal to its depth. By Lemma B.2, this leaves  $t_p$  time steps to execute the  $\text{T}$  gates of the dependency circuit. A valid gate route for the dependency circuit can be derived by executing the  $\text{T}$  gates in the order described by  $s$ . That is, if a job is executed in step  $\sigma$  in  $s$ , then the corresponding  $\text{T}$  gate is executed in step  $\sigma$  among the  $t$  available (the  $\text{CNOT}$  gates can be executed in the other time steps as described in the time limit discussion). Since  $s$  is a valid  $\text{PSP}$  solution and the dependencies among these gates match the  $\text{PSP}$  instance by Lemma B.1, this describes a valid gate route.

If the answer to the  $\text{SCMR}(A, C, t_s)$  is “yes”, we can invert this process and construct a schedule  $s$  for  $\text{PSP}(J, k, t_p)$ . We execute jobs in the order that their  $\text{T}$  gates are executed. To choose the processors for jobs, we fix a bijection between magic state vertices and processors, and execute the job on the processor corresponding to the magic state vertex used to execute the  $\text{T}$  gate. By Lemma B.2, there are  $t_p$  time steps in such a schedule. By Lemma B.1, it will satisfy the dependencies in  $J$ . Finally, since there are only  $k$  magic state qubits on  $A$ , it must satisfy the requirement that only  $k$  jobs are executed simultaneously.

## C OTHER PROOFS

### C.1 Theorem 5.1

First, let  $S = (M, t_s, R_{\text{space}}, R_{\text{time}})$  be a solution to the  $\text{SCMR}$  decision problem  $(A, C, t_s)$ . Let  $\mathcal{I}_S$  be the assignment constructed in the following way:

- Set  $\text{map}(q, v)$  if and only if  $M(q) = v$ ,
- Set  $\text{exec}(g, t)$  if and only if  $R_{\text{time}}(g) = t$ ,
- Set  $\text{path}(u, v, g, t)$  if and only if  $u$  and  $v$  are consecutive vertices (with  $u$  before  $v$ ) in  $R_{\text{space}}(g)$  and  $R_{\text{time}}(g) = t$ .

We will now show that  $\mathcal{I}_S$  satisfies  $\varphi(A, C, t_s)$  by considering each constraint:

- (1) **MAP-VALID:** By the fact that  $M$  meets our definition of a qubit map, setting the  $\text{map}(q, v)$  to true if and only if  $M(q) = v$  satisfies the **MAP-VALID** constraint.
- (2) **GATES-ORDERED:** Since  $(t_s, R_{\text{space}}, R_{\text{time}})$  is a valid gate route for  $M$ , meeting the “Logical Order” part of the definition, setting  $\text{exec}(g, t)$  if and only if  $R_{\text{time}}(g) = t$  satisfies the **GATES-ORDERED** constraint.

- (3) **DATA-SAFE**: A path variable is set to true only when it is indexed by vertices in  $R_{space}(g)$  for a gate  $g$  and a map variable is set to true only when it is indexed by a vertex in the image of  $M$ . The “Data Preservation” part of the definition of a valid gate route implies that no vertex can meet both of these criteria and that no magic state vertex can be in an  $R_{space}$  path. Therefore, **DATA-SAFE** is satisfied.
- (4) **DISJOINT**: Choose a fixed time step  $t$ . Each vertex  $u$  can be included in at most one sequence  $R_{space}(g)$  where  $g$  is such that  $R_{time}(g) = t$  by the “Disjoint Paths” condition on a valid gate route. Since the sequence  $R_{space}(g)$  is a path, each vertex appears at most once with unique vertices in adjacent positions. Thus, **DISJOINT** is satisfied.
- (5) **CNOT-ROUTED**: The **CNOT-ROUTED** constraint is satisfied because  $R_{space}$  meets the “CNOT Routing” part of the definition of a valid gate route.
- (6) **T-ROUTED**: The **T-ROUTED** constraint is satisfied because  $R_{space}$  meets the “T Routing” part of the definition of a valid gate route.

Now let  $\mathcal{I}$  be an arbitrary model of  $\varphi(A, C, t_s)$  and let  $S_{\mathcal{I}} = (M, t_s, R_{space}, R_{time})$  be derived in the following way:

- Set  $M(q) = v$  if and only if  $\text{map}(q, v)$  is set to true in  $\mathcal{I}$ .
- Set  $R_{time}(g) = t$  if and only if  $\text{exec}(g, t)$  is set to true in  $\mathcal{I}$ .
- Include  $u$  and  $v$  as consecutive vertices in  $R_{space}(g)$  if only if  $\text{path}(u, v, g, t)$  and  $\text{exec}(g, t)$  are set to true in  $\mathcal{I}$ .

We first argue that  $R_{space}$  is in fact a well-defined path with the appropriate end points for each gate  $g$ . Without loss of generality let  $g = \text{CNOT } q_i \, q_j$ . The **CNOT-START** and **DISJOINT** constraints mean that  $R_{space}(g)$  has exactly one initial vertex which appears as the first index of a path variable but not the second. Moreover, this initial vertex is  $M(q_i)$  and the second vertex is a vertical neighbor. Similarly the **CNOT-REACH-TARGET** and **DISJOINT** constraints mean that  $R_{space}(g)$  has one final vertex,  $M(q_j)$ , preceded by a horizontal neighbor. Finally **CNOT-INDUCTIVE** and **DISJOINT** constraints together mean that every other vertex  $v$  has exactly one incoming edge (from a path variable where  $v$  is the second index) and outgoing edge (from a path variable where  $v$  is the first index), ensuring a well-defined linear sequence. Thus we have established the  $R_{space}$  function meets the “CNOT Routing” and “T Routing” parts of the definition of a valid gate route.

The last nontrivial step is to show that these paths are vertex-disjoint. Suppose that some vertex  $v$  is included in  $R_{space}(g)$  and  $R_{space}(g')$  where  $R_{time}(g) = R_{time}(g')$ . By the **DISJOINT** constraint, this can only occur if  $\text{path}(u, v, g, t)$  and  $\text{path}(v, w, g', t)$  are both set to true for some vertices  $u, w$ . But then this means that  $v$  is not in the image of  $M$  and  $v \notin MS$  by the **DATA-SAFE** constraint. Therefore by the **CNOT-INDUCTIVE** and **T-INDUCTIVE** constraints,  $g = g'$ .

It is straightforward to see  $M$  is a qubit map because  $\mathcal{I}$  satisfies **MAP-VALID**. Likewise, it follows that  $(t_s, R_{space}, R_{time})$  meets the “Logical Order” and “Data Preservation” conditions of a valid gate route for  $M$  because  $\mathcal{I}$  satisfies **GATES-ORDERED** and **DATA-SAFE**, respectively.

## C.2 Theorem 6.1

LEMMA C.1. *SHORTEST-FIRST* is an  $O(\sqrt{n})$ -approximation algorithm for the Node-Disjoint Paths problem where  $n$  is the number of vertices in the input graph.

PROOF. See Kollaopoulos and Stein [28] or Erlebach [16]. □

LEMMA C.2. *When the input circuit  $C$  is restricted to be of depth 1, GREEDY-ROUTE is an  $O(\sqrt{n} \log |C|)$ -approximation algorithm for surface code routing where  $n$  is the number of vertices in the architecture.*

PROOF. We can essentially follow existing arguments [6, 8], replacing edge-disjoint paths with vertex-disjoint paths. Consider an optimal solution to  $\text{SCR}(A, C, M)$  with  $t_{\text{opt}}$  steps. There must be at

least one step where  $|C|/t_{\text{opt}}$  gates are executed. Therefore, the first application of SHORTEST-FIRST will route at least  $|C|/(\sqrt{n} \cdot t_{\text{opt}})$  of the gates by Lemma C.1, leaving a remaining circuit  $C'$ . But since  $C' \subseteq C$ , it can also be executed in  $t_{\text{opt}}$  steps, so by the same logic at least  $|C'|/(\sqrt{n} \cdot t_{\text{opt}})$  of these gates can be executed in the next step. In general, we can see that the number of unexecuted gates changes by at least a multiplicative factor of  $(1 - \frac{1}{\sqrt{n} \cdot t_{\text{opt}}})$  in each step. Thus, we need  $O(t_{\text{opt}} \sqrt{n} \log |C|)$  total steps.  $\square$

We are now ready to prove Theorem 6.1. Fix an input triple  $(A, C, M)$ . Let  $\mathcal{L} = \{l_1, \dots, l_d\}$  be the layering of  $C$  generated by GREEDY-ROUTE, and  $\text{opt}(C)$  denote the number of steps in an optimal routing solution for  $C$ . Define  $l_{\text{max}} = \text{argmax}_{l \in \mathcal{L}} \text{opt}(l)$  (where  $\text{opt}(l)$  is analogously the optimal number of time steps in a routing solution for  $l$ ). Note that

$$\sum_{i=1}^d \text{opt}(l_i) \leq d \cdot \text{opt}(l_{\text{max}}) \leq d \cdot \text{opt}(C) \quad (1)$$

Now let  $\text{gr}(C)$  be the number of time steps in the solution from GREEDY-ROUTE. Notice that  $\text{gr}(C) = \sum_{i=1}^d \text{gr}(l_i)$ . By Lemma C.2, we have that  $\text{gr}(l_i) \in O(\text{opt}(l_i) \sqrt{n} \log |l_i|)$ .

Therefore,

$$\text{gr}(C) = \sum_{i=1}^d \text{gr}(l_i) \in O\left(\sum_{i=1}^d \text{opt}(l_i) \sqrt{n} \log |l_i|\right)$$

Observe that since most one gate per layer can act on a given qubit  $|l_i| \leq q$  for all  $i$ , so we have

$$\text{gr}(C) \in O\left(\sqrt{n} \log q \sum_{i=1}^d \text{opt}(l_i)\right)$$

Now applying Eq. (1) yields our desired result:

$$\text{gr}(C) \in O(d \sqrt{n} \log q \cdot \text{opt}(C))$$

### C.3 Theorem 6.2

An interaction chain set can be constructed in time linear in the size of the circuit by stepping through the gates and adding an edge if and only if the result is still an interaction chain set. MAP-CHAIN is clearly linear time in the size of the chain, performing constant work for each qubit. STRUCT-MAP returns a function because each qubit is the first in the path (and thus assigned to a vertex under the mapping) for exactly one recursive call of MAP-CHAIN. The resulting function is injective because the image of a qubit under the mapping is chosen from the set *available* and we maintain the invariant that at this point no qubit is mapped to a vertex in *available*.

### C.4 Theorem 7.1

We will explicitly construct a mapping such that all gates are “local,” so each layer of logically parallel gates can be executed in a single step. Divide the  $2\lceil\sqrt{k}\rceil \times 2\lceil\sqrt{k}\rceil$  subgrid into  $(\lceil\sqrt{k}\rceil)^2 \geq k$  disjoint  $2 \times 2$  squares. For each  $i$  such that  $1 \leq i \leq k$ , map  $\text{LEFT}[i]$  and  $\text{RIGHT}[i]$  to the same square, with  $\text{LEFT}[i]$  in the top left corner and  $\text{RIGHT}[i]$  in the bottom right. The CNOT gates for each pair can be routed using only the bottom left vertex of the square. With these short disjoint paths, the  $n^{\text{th}}$  gate applied to a qubit can be assigned to step  $n$ , leading to optimal value equal to the depth of the circuit as desired.